

Review

Cumulative Damage and Life Prediction Models for High-Cycle Fatigue of Metals: A Review

Kris Hectors ^{1,2,*}  and Wim De Waele ² 

¹ SIM vzw, Tech Lane Ghent Science, Park/Campus A 48, BE-9052 Zwijnaarde, Belgium; wim.dewaele@ugent.be

² Laboratory Soete, Department of Electromechanical Systems and Metal Engineering, Faculty of Engineering and Architecture, Ghent University, Technologiepark 46, BE-9052 Zwijnaarde, Belgium

* Correspondence: kris.ectors@ugent.be

Abstract: Fatigue design of engineering structures is typically based on lifetime calculation using a cumulative damage law. The linear damage rule by Miner is the universal standard for fatigue design even though numerous experimental studies have shown its deficiencies and possible non-conservative outcomes. In an effort to overcome these deficiencies, many nonlinear cumulative damage models and life prediction models have been developed since; however, none of them have found wide acceptance. This review article aims to provide a comprehensive overview of the state-of-the art in cumulative damage and lifetime prediction models for endurance based high-cycle fatigue design of metal structures.

Keywords: cumulative fatigue damage; fatigue damage accumulation; cumulative damage rules; load interaction effects; fatigue life predictions; high-cycle fatigue; damage model; failure prediction



Citation: Hectors, K.; De Waele, W. Cumulative Damage and Life Prediction Models for High-Cycle Fatigue of Metals: A Review. *Metals* **2021**, *11*, 204. <https://doi.org/10.3390/met11020204>

Received: 27 December 2020

Accepted: 18 January 2021

Published: 22 January 2021

Publisher's Note: MDPI stays neutral with regard to jurisdictional claims in published maps and institutional affiliations.



Copyright: © 2021 by the authors. Licensee MDPI, Basel, Switzerland. This article is an open access article distributed under the terms and conditions of the Creative Commons Attribution (CC BY) license (<https://creativecommons.org/licenses/by/4.0/>).

1. Introduction

The concept of cumulative fatigue damage calculation dates back to the 1920s when the idea of linear fatigue damage accumulation was first published by [1]. In 1945, the same hypothesis was formulated by Miner [2], which is now widely known as the Palmgren–Miner rule, the linear damage rule (LDR), or simply as Miner's rule. Miner's rule is based on the hypothesis that the fatigue damage is equal to the accumulated cycle ratio, expressed as

$$D = \sum \frac{n_i}{N_i} \quad (1)$$

D is the damage (where D equal to unity theoretically corresponds to failure), and n_i and N_i are the number of applied cycles and the number of cycles to failure for the i_{th} constant amplitude stress level σ_i , respectively. Miner's rule has become the industry standard for fatigue design of metal structures based on the endurance approach due to its intrinsic simplicity. It has been adopted in leading design standards for steel structures such as EN 1993-1-9:2005 [3], DNVGL-RP-C203:2016 [4], and BS 7608:2014 [5].

A comprehensive overview and critical review of different fatigue testing programs and their results was published by Schütz [6]. The testing programs revealed that large discrepancies exist between experimental lifetimes and these predicted by Miner's rule. Lifetime predictions tend to be conservative for low-to-high ($\sigma_1 < \sigma_2$) loading sequences and non-conservative for high-to-low loading sequences ($\sigma_1 > \sigma_2$). For random load spectra, factors of 10 and more on the non-conservative side were not uncommon. Thus, despite its wide use, Miner's rule is known to exhibit a number of drawbacks. The main deficiencies are its load level independence, load sequence independence, and lack of accounting for load interaction effects due to crack tip plasticity [7]. Schijve [8] also mentions its inability to account for the contribution to fatigue damage of cycles that have

a stress amplitude below the endurance limit, which has been addressed in two ways. The first is referred to in literature as the modified Miner's rule where the S–N curve is simply extended from the knee point with the same slope as the original curve. The second method is Haibach's [9] approach, which suggests to extend the S–N curve from the knee point with a slope equal to $-1/(2m - 1)$. The parameter m is the slope factor of the S–N curve when expressed as $\sigma = bN^{-1/m}$. It has however been shown that both methods tend to be non-conservative in most variable amplitude experiments (e.g., Sonsino et al. [10], Sonsino et al. [11], and Schoenborn et al. [12]). To overcome this, He et al. [13] proposed the cumulative fatigue damage saturated model in which a critical number of cycles of below the fatigue limit in one block exists. When the value is exceeded, the remaining cycles below the fatigue limit become harmless. Liu et al. [14] proposed a modified Miner damage accumulation algorithm for both pure and corrosion fatigue that considers load interaction effects by introducing the effective stress ratio concept R_{eff} from the Willenborg–Chang fracture mechanics model [15] into Miner's rule.

In order to overcome the shortcomings inherent to the linear damage accumulation rule, a wide range of nonlinear damage accumulation models has been developed. In 1998, a comprehensive review on cumulative fatigue damage and life prediction theories was published by Fatemi and Yang [7]. Since then, a significant number of new nonlinear damage models have been published. A number of review papers have been published discussing some of the models. Santecchia et al. [16] published a review on fatigue life prediction methods for metals, Bandara et al. [17] on fatigue failure predictions for very high-cycle fatigue, and Jimenez-Martinez [18] on fatigue damage assessment of offshore structures under stochastic loadings. However, the topic of nonlinear cumulative damage models for endurance based fatigue design has not been thoroughly reviewed. The aim of this paper is to present a comprehensive review of nonlinear fatigue damage accumulation models primarily published after 1998 to extend the work of Fatemi and Yang [7]. The present review mainly focuses on high-cycle fatigue, but models developed for low-cycle fatigue that formed the basis for future works on high-cycle fatigue are also considered. A few models developed before 1998 that are fundamental as an introduction to recent works are also included. Fatemi and Yang [7] categorized the reviewed theories and models in six categories: (a) linear damage rules, (b) nonlinear damage curve and two-stage linearization methods, (c) life curve modification methods, (d) approaches based on crack growth concepts, (e) continuum damage mechanics models, and (f) energy-based theories. Note that there is no clear boundary between these categories and other categorizations have also been proposed (e.g., Zhu et al. [19]). For this review article, the authors decided to use the categorization proposed by Fatemi and Yang [7]. Damage models that may fall into different categories are assigned a category based on their theoretical basis or their role in the development of subsequent models. In this article, cumulative damage models based on crack growth concepts are not discussed as the focus of the review lies on cumulative damage models for high-cycle fatigue design based on the endurance approach. The authors do not claim this review to be exhaustive but it constitutes a representative overview of the state of the art.

2. Nonlinear Damage Curve and Two-Stage Linearization Models

2.1. Historical Introduction

In 1948, Richart and Newmark [20] introduced the damage curve concept correlating damage to the cycle ratio with the goal to overcome the shortcomings of the LDR. They speculated that the D - r curves (with r the cycle ratio n/N) should be dependent on the stress level. Based on this concept, as well as empirical evidence, the nonlinear damage rule (NLDR) was proposed by Marco and Starkey [21]. The NLDR expresses the damage as a power function which is load-dependent:

$$D = \sum \left(\frac{n_i}{N_i} \right)^{x(\sigma_i)} \quad (2)$$

The value of the exponent x is a function of the stress amplitude. Obviously Miner's rule is a special case of Equation (2) where x is equal to one for all σ_i . The damage curve concept is illustrated in the right part of Figure 1. It shows how the damage is accumulated in a D - r diagram for both the LDR and the NLDR. Figure 1 shows that the predicted number of cycles to failure is lower in the case of nonlinear damage accumulation as the accumulated $n/N \approx 0.7$ when the damage $D = 1$, while $n/N = 1$ when the damage $D = 1$ in the case of linear damage accumulation.

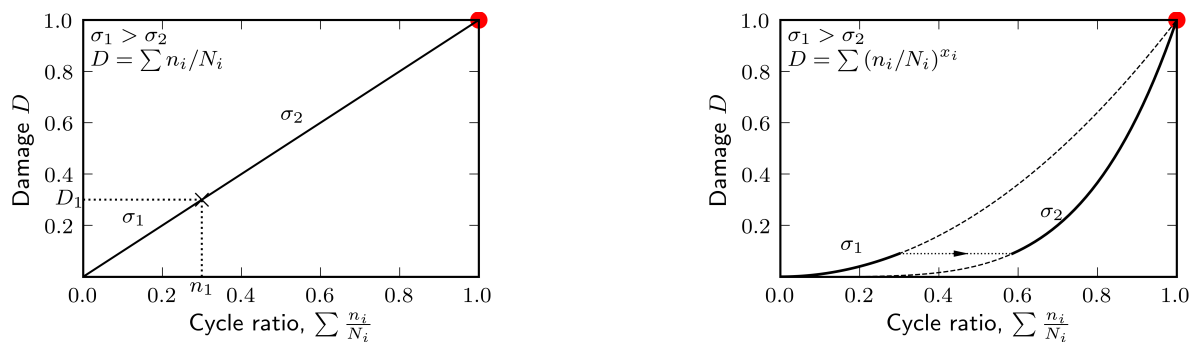


Figure 1. Linear damage rule (LDR) (left) versus nonlinear damage rule (NLDR) (right) for a high-to-low loading sequence. The red dot indicates the point of failure.

Langer [22], and later Grover [23], suggested that damage accumulation should be analyzed using two LDRs. In 1960, Grover suggested a two-stage linear damage rule based on observations from a fracture mechanics viewpoint. The first stage represents the crack initiation stage and the second stage represents crack propagation. Grover's work was qualitative and did not provide a quantitative formulation for separation of the total life into initiation and propagation stages. In 1966, Manson [24] proposed the double linear damage rule (DLDR) based on Grover's work. In 1967, Manson et al. [25] changed the viewpoint of the DLDR such that the concept of crack initiation and propagation in the literal sense is altered to represent two effective phases of the fatigue process. The alteration implied that the DLDR became material and load dependent, which overcame some of the limitations of their original proposal. Manson and Halford [26] experimentally compared the DLDR with Miner's rule and found that Miner's rule resulted in an average overestimation of 37% compared to an average overestimation of 12% for the DLDR.

Shortly after proposing the DLDR, Manson and Halford [26] proposed the damage curve approach (DCA) which is also based on the damage curve concept of Marco and Starkey [21]. Marco and Starkey [21] did not provide a specific functional form for the exponent $x(\sigma_n)$ which severely limits its practicality. Based on an empirically formulated effective crack growth model, Manson and Halford [26] proposed an analytical formulation for the damage curve. The damage model for a multi-level loading sequence can be expressed as

$$\left[\left[\left[\left(\frac{n_1}{N_1} \right)^{\alpha_{1,2}} + \frac{n_2}{N_2} \right]^{\alpha_{2,3}} + \frac{n_3}{N_3} \right]^{\alpha_{3,5}} + \dots + \frac{n_{i-1}}{N_{i-1}} \right]^{\alpha_{i-1,i}} + \frac{n_i}{N_i} = 1 \quad \text{with} \quad \alpha_{i-1,N_i} = \left(\frac{N_{i-1}}{i} \right)^{0.4} \quad (3)$$

where $1, 2, \dots, i-1, i$ are the sequence numbers of the load components. Manson and Halford [26] found that the difference between the DLDR and DCA was relatively small for two-level and three-level block loading tests. This was not unexpected as the DLDR should be regarded as a linearization of the damage curve concept. However, for more realistic loading conditions a larger difference is expected, as the result of the DLDR is not affected by the load changes within a single phase whereas the DCA is affected by all changes in the load sequence.

An experimental study of Costa et al. [27] on the fatigue behavior of AA6082 aluminum alloy friction stir welds subjected to variable amplitude loading compared Miner's rule with the DLDR. They concluded that DLDR was significantly more accurate, but both were very

non-conservative for fully reversed loading conditions ($R = -1$). Inoma et al. [28] implemented the DLDR and Miner's rule for fatigue life prediction of offshore drilling top-drive tie rods and found that Miner's rule consistently overestimated the fatigue lives and that better estimates were obtained with the DLDR. In general the DLDR is found to be a considerable improvement over Miner's rule since the required input is the same.

The original DCA model of Manson and Halford [26] was empirically defined based on results from two-level load sequences that did not involve very small values of n_1/N_1 . Manson and Halford [29] noticed that the drop of n_2/N_2 for a very small n_1/N_1 is very rapid for high-low loading with $N_2 \gg N_1$. In order to achieve more accurate results at very low n_1/N_1 , a term was added to the original DCA equation which is of large significance for low values of n_1/N_1 but relatively small for larger values. They refer to this model as the double damage curve approach (DDCA). It is a combination of the most accurate parts of the DLDR and DCA. Figure 2 shows the DLDR, DCA and DDCA for three values of N_{ref}/N_i with N_{ref} a reference life level.

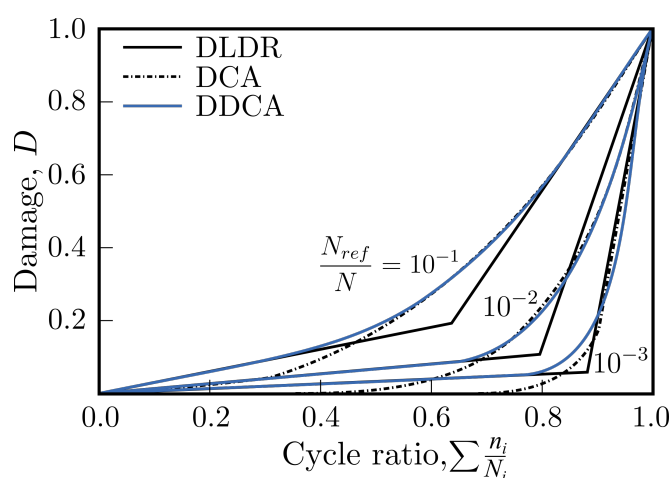


Figure 2. Double damage curve approach (DDCA) blends with the double linear damage rule (DLDR) at low cycle ratios and with the damage curve approach (DCA) at high cycle ratios [29].

The DLDR, DCA, and DDCA models all possess similar characteristics as they are load level-dependent, but do not account for load interaction and cycles with an amplitude below the fatigue limit [7]. The most common method to account for load interactions is through the use of an interaction factor that depends on the load ratio. This was first proposed by Corten and Dolan [30] in 1956. Based on hundreds of constant amplitude and two-level block loading tests on cold-drawn steel wires they proposed a phenomenological cumulative damage model that is expressed as

$$D = m r n^a \quad (4)$$

here m is the number of damage nuclei, r is the damage propagation rate coefficient which is a function of the stress condition, n is the number of applied cycles, and a is a material constant. The damage model is based on the assumption that damage occurs as the nucleation of microscopic voids that ultimately form cracks. The rate at which damage takes place, increases with the number of applied cycles and the stress amplitude. Furthermore, damage can also propagate at stress levels that are lower than the stress required to initiate damage. Based on two-level block loading experiments, Corten and Dolan [30] established an empirical relation between the stress dependent ratio $R = r_1/r_2$, the damage exponent a and the stress ratio through a material property d . The empirical relationship is given by $R^{1/a} = (\sigma_2/\sigma_1)^d$ and has been used to determine Equation (5) where N_g is the total number of cycles to failure. Failure is assumed to occur when D reaches unity. The parameter d represents the slope of a linear curve in a $\log(R^{1/a}) - \log(\sigma_2/\sigma_1)$ diagram, where $R = r_1/r_2$ and can be determined experimentally.

$$N_g = \frac{N_1}{\sum \alpha \left(\frac{\sigma_i}{\sigma_1} \right)^d} \quad (5)$$

The life prediction model expressed by Equation (5) takes load interaction effects into account through the load ratio (σ_i/σ_1).

2.2. Models Based on the Damage Curve Approach

Chen et al. [31] studied the effects of sequential loading on fatigue damage of 304SS stainless steel subjected to tension-compression followed by torsion, torsion followed by tension-compression, in-phase loading followed by 90° out-of-phase loading, and 90° out-of-phase loading followed by in-phase loading. Fatigue tests with a number of cycles ranging from 10^3 – 10^4 were performed and several fatigue damage rules, including Miner's rule, the DLDR, and the DCA, were evaluated. All models were found to yield non-conservative predictions. It was hypothesized that additional hardening by the sequential loading influenced the fatigue resistance of the material. Considering the experimental results, a non-proportionality function J was introduced in the DCA model exponent α to consider the loading path in the sequential loading. The exponent α for a two-level block loading was redefined as

$$\alpha = \left(\frac{1}{1 + \beta J} \right) \left(\frac{N_1}{N_2} \right)^{0.4} \quad \text{with} \quad J = \frac{1.57}{T \varepsilon_{1,max}} \int_0^T |\sin \zeta(t)| \varepsilon(t) dt \quad (6)$$

where $\varepsilon_1(t)$ and $\zeta(t)$ are the absolute value and the angle respectively, of the maximum principal strain at time t . T and $\varepsilon_{1,max}$ are the time for a cycle and the maximum value of $\varepsilon(t)$ in a cycle [32]. Due to the small number of tests and relatively large scatter in the experimental results, further validation is required. Preliminary results did show an improvement over existing models.

Xu et al. [33] identified the need for the DCA to account for load interaction effects. They suggested that parameter $\alpha_{i-1,i}$ of the DCA model (see Equation (3)) could be modified to include load amplitude and effective stress related to the loading. Based on this suggestion and the works of Corten and Dolan [30] and Freudenthal and Heller [34], Gao et al. [35] suggested to modify the parameter $\alpha_{i-1,i}$ by adding a term that represents the minimum ratio of the applied stress amplitudes. The parameter $\alpha_{i-1,i}$ becomes

$$\alpha_{i-1,i} = \left(\frac{N_{i-1}}{N_i} \right)^{0.4 \min \left\{ \frac{\sigma_{i-1}}{\sigma_i}, \frac{\sigma_i}{\sigma_{i-1}} \right\}} \quad (7)$$

Gao et al. [35] reported that nearly 80% of their modified DCA model predictions are better than those of the original Manson–Halford DCA model for two-level block loading tests on C45 and 16Mn steel.

Yuan et al. [36] argue that, except accounting for load sequence and load interaction effects, an accurate fatigue damage model should also account for strength degradation. Therefore, they further modified the DCA model of Gao et al. [35] to account for residual strength degradation by introducing a residual strength degradation function. The damage induced by the n_i applied cycles at stress amplitude σ_i can be determined as

$$D_i = \gamma \left(\frac{n_i}{N_i} \right) \left(\frac{N_{i-1}}{N_i} \right)^{0.4 \min \left\{ \frac{\sigma_{i-1}}{\sigma_i}, \frac{\sigma_i}{\sigma_{i-1}} \right\}} \quad \text{with} \quad \gamma = \exp \left[\alpha \left(\frac{1}{A} - 1 \right) \right] \quad (8)$$

where α is a material coefficient that can be obtained from experimental data, A is the residual strength degradation coefficient that reflects the relationship between the strength degradation and the fatigue damage accumulation.

In 2019, Zhou et al. [37] proposed a new cumulative damage model that is a combination of a damage curve approach based model and the Corten–Dolan model without clear

physical motivation. Take note that verification has been based on only a single experiment. For a multi-level loading sequence the model is expressed as

$$D = \left\{ \left[\left(\frac{n_1}{N_1} \left(\frac{N_1}{N_2} \right)^{\alpha \left(\frac{\sigma_{max,1}}{\sigma_f} \right)} \right) + \frac{n_2}{N_2} \right] \left(\frac{N_2}{N_3} \right)^{\alpha \left(\frac{\sigma_{max,2}}{\sigma_f} \right)} + \dots + \frac{n_{i-1}}{N_{i-1}} \right\} \left(\frac{N_{i-1}}{N_i} \right)^{\alpha \left(\frac{\sigma_{max,i-1}}{\sigma_f} \right)} + \frac{n_i}{N_i} \quad (9)$$

$\sigma_{max,i}$ is the maximum stress at the i_{th} stress level, σ_f is the fatigue limit and α_i has the same meaning as in Equation (3).

2.3. Nonlinear Damage Accumulation Models Based on the S–N Curve

Kwofie and Rahbar [38,39] proposed a new concept based on the Basquin equation, named the fatigue driving stress (FDS). They suggested that the FDS is the driver of fatigue damage and that it can be used to predict the residual fatigue life of a structure subjected to variable amplitude loading. The FDS increases in a nonlinear fashion with each cycle, cumulatively damaging the material. When a critical value of FDS is reached, failure is assumed to occur. The critical fatigue driving stress is independent of the applied stress or any load interactions. The value of the FDS attained by the previous loads is used to determine an equivalent life-fraction that would be expended by the current load only and is used to predict the remaining life. The FDS due to an applied cyclic stress σ_i can be expressed as

$$S_{D_i} = \sigma_i N_i^{-\frac{b n_i}{N_i}} \quad (10)$$

where n_i and N_i have their usual meaning and b is the fatigue strength exponent. It can be shown that the cumulative fatigue damage for variable amplitude loading according to the model of Kwofie and Rahbar [39] can be formulated as shown in Equation (11). The full derivation hereof is omitted for the sake of brevity, the reader is referred to the work in [39].

$$D = \sum \frac{n_i \ln(N_i)}{N_i \ln(N_1)} \quad (11)$$

here N_1 is the fatigue life for the first applied load that initiates fatigue damage. The ratio $\ln(N_i)/\ln(N_1)$ accounts for the load sequence and interaction effects. Although the FDS defined in Equation (10) is clearly a nonlinear function, the damage accumulation function, Equation (11), is a piece-wise linear function. Notice that for $N_i = N_1$, Equation (11) reduces to the linear damage rule. In general, the remaining life for variable amplitude block loading can be calculated as

$$\frac{n_i}{N_i} = \frac{\left(1 - \frac{n_1}{N_1}\right) \ln(N_1) - \frac{n_2}{N_2} \ln(N_2) - \frac{n_3}{N_3} \ln(N_3) - \dots - \frac{n_{i-1}}{N_{i-1}} \ln(N_{i-1})}{\ln(N_i)} \quad (12)$$

In 2015, Zuo et al. [40] proposed a new damage model based on the fatigue driving stress concept of Kwofie and Rahbar [39]. The authors of this paper are of the opinion that the proposed damage model is identical to the one of Kwofie and Rahbar [39] (i.e., Equation (11)) and that the remaining lifetime function derived from it contains an error, which if fixed is again identical to the remaining lifetime function of Kwofie and Rahbar [39] (i.e., Equation (12)).

A modification for the FDS-based model of Kwofie and Rahbar [39] was also proposed by Zhu et al. [41]. By adding an interaction factor that is a function of subsequent stress levels, they aim to account for load interaction effects. The modified remaining lifetime function is described as

$$\frac{n_i}{N_i} = \left(1 - \frac{n_1}{N_1} - \frac{n_2}{N_2} - \dots - \frac{n_{i-1}}{N_{i-1}}\right) \left(\frac{\ln(N_1)}{\ln(N_i)}\right)^{\frac{\sigma_{i-1}}{\sigma_i}} \quad (13)$$

In 2017, Aeran et al. [42,43] expressed the need for a model that is based on commonly available S-N curves. They reasoned that none of the available models at that time were readily applicable because they require the determination of extra material parameter(s) or a modification of the S-N curve. They proposed a damage model that is solely based on S-N curves without the need for additional parameters. A new damage index was proposed that is given in Equation (14). The model parameter δ_i can be determined using available S-N curves as it only depends on N_i . It can thus be calculated for any design detail of which the S-N curve is available [42]. The fatigue damage D can be represented by the absolute value of the proposed damage index D_i , i.e., $D = |D_i|$.

$$D_i = 1 - \left[1 - \frac{n_i}{N_i}\right]^{\delta_i} \quad \text{with} \quad \delta_i = \frac{-1.25}{\ln(N_i)} \quad (14)$$

For a more reliable estimation of fatigue life under variable amplitude loading, Aeran et al. [42] also proposed a new damage transfer concept. To account for load sequence and load interaction effects, a new interaction factor μ was proposed. For loading block $i + 1$, the interaction factor is calculated as

$$\mu_{i+1} = \left(\frac{\sigma_i}{\sigma_{i+1}}\right)^2 \quad (15)$$

The proposed damage transfer concept is based on the use of fatigue damage evolution curves and the proposed load interaction factor μ . The damage for a given stress level can be determined using the damage evolution curve of the considered material, i.e., for a material that is subjected to n_i cycles with a stress amplitude σ_i , the fatigue damage can be determined using Equation (14). If the same material is subsequently loaded for n_{i+1} cycles with a stress amplitude σ_{i+1} , the damage can be transferred from σ_i to σ_{i+1} by using the interaction factor μ_{i+1} together. An effective number of cycles $n_{(i+1),eff}$ is determined that corresponds to σ_{i+1} using Equation (16). Physically, this means that the damage state of the material does not change while transferring the loading state from one stress level to the next.

$$n_{(i+1),eff} = N_{i+1} \left[1 - (1 - D_i)^{\frac{\mu_{i+1}}{\delta_{i+1}}}\right] \quad (16)$$

A number of $n_{(i+1),eff}$ cycles at σ_{i+1} would result in the same damage D_i , had it been present from the start. The total number of cycles at loading cycle $i + 1$ can be calculated using Equation (17). The cumulative damage after loading step $i + 1$ can then be calculated using Equations (18) and (19).

$$n_{(i+1),total} = n_{(i+1),eff} + n_{(i+1)} \quad (17)$$

$$D_{i+1} = 1 - \left[1 - \frac{n_{(i+1),total}}{N_{i+1}}\right]^{\delta_{i+1}} \quad (18)$$

$$D = |D_{i+1}| \quad (19)$$

The method is illustrated in Figure 3; for a flowchart of the damage transfer concept proposed by Aeran et al. [42], reference is made to their original work. As the proposed model can also be applied to design details by using the appropriate S-N curve defined in design standards, it can easily be implemented by practicing engineers.

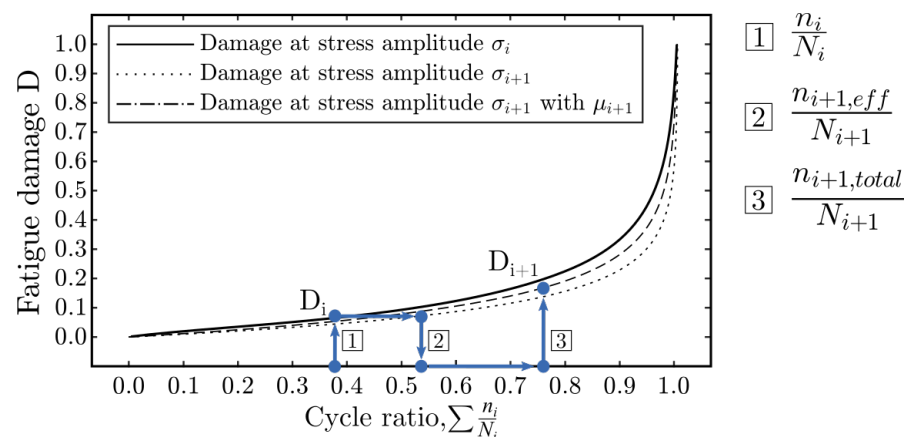


Figure 3. Graphical presentation of the damage transfer concept proposed by Aeran, adopted from the work in [42].

Similar to Kwofie and Rahbar [39], Si-Jian et al. [44] proposed a new damage accumulation model that only requires an S–N curve as input. The damage model is based on Miner’s rule and the Basquin equation. Si-Jian et al. [44] derived the following function for the cumulative damage:

$$D = 1 - \left[\left[\left(\frac{n_1}{N_1} \right)^{\frac{\sigma_2}{\sigma_1}} + \frac{n_2}{N_2} \right]^{\frac{\sigma_3}{\sigma_2}} + \dots + \frac{n_{i-1}}{N_{i-1}} \right]^{\frac{\sigma_i}{\sigma_{i-1}}} + \frac{n_i}{N_i} \quad (20)$$

Theil [45] proposed a new fatigue life prediction method based on linearized damage growth curves in a double linear S–N diagram where the S–N curve corresponds to failure. The goal of the model is to account for the effects of overload blocks with stress levels around the 0.2% yield strength level and slightly (~10%) above. The lifetime prediction method is based on an iterative calculation that is explained based on Figure 4. Assume the four-level block loading shown in Figure 4 characterized by the (σ_{ai}, n_i) pairs shown. The linear dash-dotted lines represent the linearized damage growth curves, their slope depends on the corresponding stress. Failure occurs when the fatigue life associated with the the damage growth curve of the current stress level is reached, i.e., N_i for the i_{th} load block. Theil [45] assumed that damage growth is linear for a constant amplitude. In Figure 4, the line OW_1 represents the damage growth curve at the first load level. The equation of this line can be written as

$$\sigma_1 = w_1 N_1 \rightarrow w_1 = \frac{\sigma_1}{N_1} = \frac{\zeta_{11}}{n_1} \quad \text{with} \quad \zeta_{11} = w_1 n_1 \quad (21)$$

where n_1 and N_1 are the number of applied cycles and the fatigue life at σ_{a1} respectively; ζ_{11} is the stress level corresponding to n_1 on the current damage curve; and w_1 is the slope of the damage curve OW_1 . The calculation for the following load blocks is continued in the same way. Note that the damage growth for subsequent load blocks occurs on a damage curve OW'_i that is parallel to the curve OW_i . To determine the remaining fatigue live at a certain stress amplitude, the intersection between the relevant linearized damage growth curve and the S–N curve has to be determined. This is illustrated for the fourth load block by the blue area in Figure 4.

Theil [45] validated the proposed model to experimental data available in literature of a fine grain low alloy structural steel, aluminum alloys, and austenitic steel bolt joints. He found that the model estimations are better than those obtained with Miner’s rule. Theil [45] also notes that better lifetime estimations could be obtained by using nonlinear damage growth curves, but this would increase the number of required parameters and thus reduce its applicability for practical engineering.

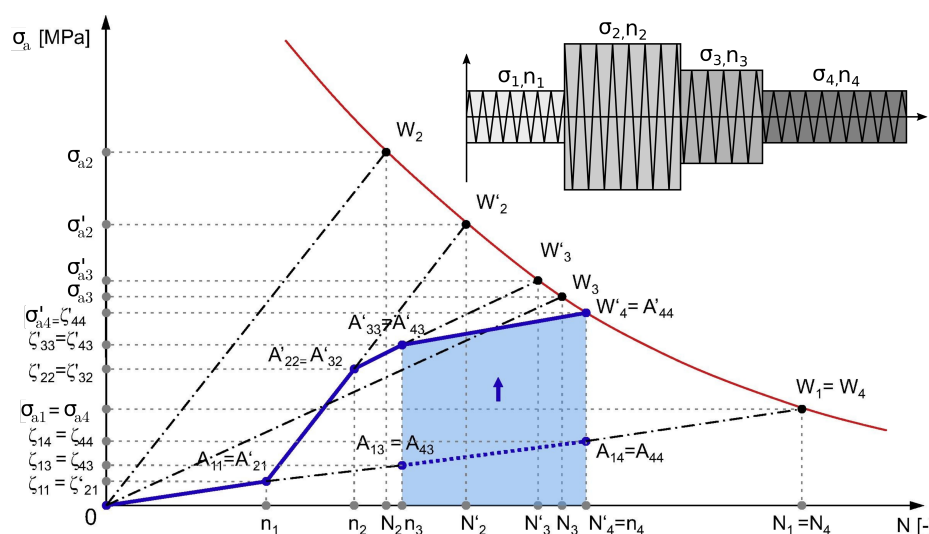


Figure 4. Illustration of the linearized damage growth curve approach proposed by Theil for fatigue life prediction in case of a four-level block loading. Figure adopted from the work in [45].

3. Life Curve Modification Models

Life curve modification models modify the S–N curve to account for different effects, such as load sequence and interaction effects. Two types of life curve modification models can be distinguished. The first type is based on the models of Corten and Dolan [30] and Freudenthal and Heller [34]. The second type is based on the concept of isodamage lines first mentioned in the studies of Hunter and Fricke [46].

3.1. Life Curve Modification Models Based on the Models of Corten–Dolan and Freudenthal–Heller

The models of Corten–Dolan [30] and Freudenthal–Heller [34] both represent a clockwise rotation of the S–N curve around a reference point. Although the models are similar in application, they are based on different ideas and consequently use a different reference point for the rotation. Corten and Dolan introduced the idea that larger numbers of damage nuclei which are produced at high stress amplitudes will cause an increased growth rate of damage nuclei at subsequent lower stress levels [47]. Freudenthal and Heller [34] suggested that the damage rate is independent of the load level [7]. For the Corten–Dolan model, the point corresponding to the highest stress amplitude in the load spectrum is selected as the reference point. The Freudenthal–Heller model defines the reference point as the stress level where the low-cycle fatigue region transitions to the high-cycle fatigue region, which is mentioned to be between 10^3 and 10^4 cycles.

Leipholz agreed with the idea that life-reducing interaction effects between cycles of variable amplitude could be accounted for by modifying the original S–N curve. Leipholz [48–50] introduced a new model in which the original S–N curve is replaced with a modified curve $S - \hat{N}_i$, which accounts for load interaction effects. The model is expressed as

$$N = \left[\sum_{i=1}^k \frac{\beta_i}{\hat{N}_i} \right]^{-1} \quad \text{with} \quad \beta_i = \frac{n_i}{N_i} \tag{22}$$

N is the total accumulated fatigue life and \hat{N}_i is the modified life at stress amplitude σ_i . Typically, the original and modified curves converge at high loading levels but deviate at lower loading levels. Fatigue life predictions using the Leipholz model have been found reasonably accurate, a reduced number of greatly non-conservative results was observed when compared to Miner’s rule predictions [51].

The parameters required to account for the interaction effects defined by Freudenthal and Heller are difficult to relate to experiments. On the other hand, the parameter d in the Corten–Dolan model can be determined from simple two-level loading tests. Therefore,

the Corten–Dolan model has found more use in literature than the Freudenthal–Heller model. The empirically determined parameter d defined by Corten and Dolan [30] as a material parameter (see Equation (5)) has been studied by many researchers. Spitzer and Corten [52] proposed to determine the slope of the modified S–N curve (i.e., the parameter d) from the average slope of a few S–N curves determined from two-level block loading tests. They validated their approach with fully reversed bending tests ($R = -1$) on 2024-T4 and 7075-T6 aluminium alloy wire.

It has been shown that the Corten–Dolan model is suitable for a wide range of applications with good precision [53]. However, lifetime estimations are strongly dependent on the value of the exponent d . For steels, Rao et al. [54] reported that d ranges from 6.2 to 6.9 with a mean value of 6.57. Peng et al. [55] report recommended values of 4.8 for high strength steels and 5.8 for other materials. The determination of the exponent d is (semi-)empirical, requires many experiments and it lacks theoretical basis according to Zhu et al. [19]. Jiao et al. [56] performed three experiments on spherical welded joints from Q235B steel and calculated values of 3.39, 18.69, and 27.09 for d indicating the difficulty of obtaining a consistent value. The theory of Spitzer and Corten [52] that d could be determined from two-level block loading and used for multi-level block loading conditions was disproven by Marsh and Mackinnon [57] as they showed that it often leads to unsafe predictions. Nonetheless, the effects of load interaction and low-amplitude loading are considered in the Corten–Dolan model, giving it a major advantage over Miner’s rule. Recently, He et al. [13] have shown that the Corten–Dolan model can be used to estimate the fatigue life for various multi-pass welded stainless steels whose S–N curves exhibit bilinear characteristics, including load spectra below the fatigue limit.

In 2012, Zhu et al. [19] suggested a new way to determine the exponent d . They suggested that d is in fact a function of the applied stresses instead of a material constant, which is in agreement with other studies (e.g., Zhao [53], Yang et al. [58], Zhu et al. [59]). The modified parameter d is proposed as

$$d(\sigma_i) = \mu \frac{\sigma_1^\lambda \delta_f^{1-\lambda}}{\sigma_i} \quad (23)$$

μ is a material constant, λ is a factor that accounts for load sequence effects with $0 < \lambda < 1$ ($\lambda = 0$ for constant amplitude loading as there is no load interaction). For simplicity, the value of λ can be estimated as $\lambda = n_1/N_1$. The parameter δ_f is the initial strength of the specimen which can be determined experimentally. Zhu et al. [19] suggest that δ_f can be estimated (for metals only) as $\delta_f \approx \sigma_b + 350$ MPa with σ_b the ultimate tensile strength. The authors of this paper are of the opinion that the suggested estimation is not physically sound as the initial strength cannot be larger than the ultimate tensile strength. Even if σ_b would be equal to the yield stress, this expression does not make sense. The ratio δ_f/σ_i characterizes the effect of material properties on the fatigue life; the ratio σ_1/σ_i is the interaction factor. Experimental results of high-to-low and low-to-high block load sequences on C45 and 16 Mn steels were compared to predicted fatigue lives. Results showed that the proposed model provides better lifetime predictions than Miner’s rule for two-level block loading conditions. Although Zhu et al. [19] stated that it can be used for multi-level block loading, no validation based on multi-level block loading experiments has been reported.

Gao et al. [60] proposed a new expression for the exponent d , shown in Equation (24). It is based on a criterion proposed by Zhu et al. [59] which states that fatigue failure is influenced by the combined effect of the degree of damage and the stress conditions and can be described by an exponential function of the cycle ratio and loading ratio. Gao et al. [60] further modified the form proposed by Zhu et al. [59] with the addition of a material parameter γ . The parameter γ is a material constant that can be derived from experimental data and the chosen failure criterion (e.g., $n/N = 1$).

$$d = \exp \left[\left(\frac{n_i}{N_i} \right)^{\sigma_i / \sigma_{max}} \right] + \gamma \quad (24)$$

Gao et al. [60] compared their model to the original Corten–Dolan model for normalized C45 steel, normalized 16Mn steel and hot-rolled 16Mn steel. The lifetime prediction errors for the proposed model were all within a 50% error margin which was not the case for predictions made using Miner’s rule. They also compared their model to that of Zhu et al. [19]; fatigue life predictions of both models were found to be similar but the average error is smaller for the model of Gao et al. [60].

Expression (24) was further modified by Xue et al. [61] to account for the effect between stress ratios of consecutive load blocks:

$$d = \frac{\sigma_i}{\sigma_{i-1}} \left[\exp \left(\frac{n_i}{N_i} \right)^{\sigma_i / \sigma_{max}} + \gamma \right] \quad (25)$$

This equation was again modified by Liu et al. [62]

$$d = \left(\frac{\sigma_i}{\sigma_{i-1}} \right)^k \left[\exp \left(\frac{n_i}{N_i} \right) + \gamma \right] \quad (26)$$

The exponent k is a natural integer. Liu et al. [62] extensively validated their model to two-level and multi-level block loading data available in literature and compared it to the models of Gao et al. [60] and Xue et al. [61]. They showed that the lifetime estimations based on their model are significantly better than the other two. It should however be noted that no clear guidance on the value of the exponent k is given. Both $k = 2$ and $k = 3$ gave good results, they reported that further research is required to determine the best value.

3.2. Life Curve Modification Models Based on Isodamage Lines

The easiest way to assess the fatigue life of a damage free structure is through the use of an S–N curve. This concept can be translated to a remaining lifetime assessment following a certain number of applied load cycles. After n_i cycles with amplitude σ_i , the residual fatigue life equals N_{iR} . The concept of isodamage lines is based on the assumption that the S–N curve of a material corresponds to a state of 100% fatigue damage, while combinations of stresses and cycles (σ_i, n_i) with identical damage values fall on smooth curves when plotted. Subramanyan [63] introduced a set of straight isodamage lines in an S–log(N) diagram, which converge near the knee-point of the S–N curve (see Figure 5). The damage is defined as the ratio of the slope of an isodamage line to the limiting value of the slope of the S–N curve as shown in Equation (27). Expressing the damage as a logarithmic function of the load cycles implies that the number of cycles required to cause a certain amount of damage increases when the stress amplitude decreases, and vice versa. This means that the model accounts for the increased lifetime observed for high-to-low block loading sequences and for the decreased lifetime observed for low-to-high block loading sequences.

$$D_i = \frac{\tan(\theta_i)}{\tan(\theta_f)} = \frac{\log(N_f) - \log(N_i)}{\log(N_f) - \log(n_i)} \quad (27)$$

Here, N_f is the number of cycles to failure at the knee point of the S–N curve, n_i is the number of cycles with stress amplitude σ_i applied in load step i and N_i is the fatigue life for a constant stress amplitude σ_i . When a new loading step is applied at stress amplitude σ_{i+1} , the isodamage line is followed to the new stress amplitude. It is then possible to define an equivalent number of cycles $n_{i,i+1}$ at stress amplitude σ_{i+1} for which the damage is the same as after n_i cycles at σ_i . The equivalent number of cycles $n_{i,i+1}$ can be calculated as

$$n_{i,i+1} = N_{i+1} \left(\frac{n_i}{N_i} \right)^{\alpha_i} \tag{28}$$

with

$$\alpha_i = \frac{\log(N_f) - \log(N_{i+1})}{\log(N_f) - \log(N_i)} = \frac{\sigma_{i+1} - \sigma_f}{\sigma_i - \sigma_f} \tag{29}$$

The residual fatigue life $N_{(i+1)R}$ at loading step $i + 1$ becomes

$$N_{(i+1)R} = N_i - n_{i,i+1} \tag{30}$$

This procedure is illustrated in Figure 5.

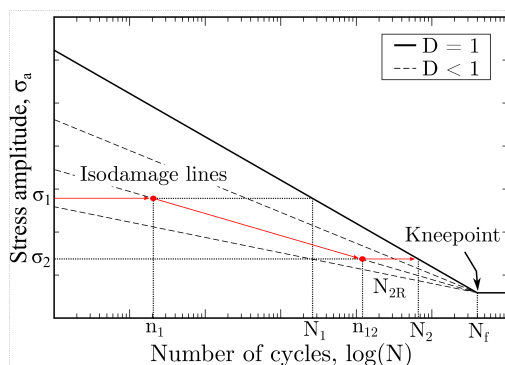


Figure 5. Isodamage path for a two-level block loading sequence according to Subramanyan [63].

Hashin and Rotem [64] proposed a different approach based on the concept of isodamage lines. They suggested that isodamage lines should converge at the point where the S–N curve intersects with the S-axis as shown in Figure 6. Notice that the isodamage lines defined by Hashin and Rotem [64] intersect the N-axis for $\sigma_a = 0$. This implies that the fatigue life is lower for a two-stage block load sequence, with $\sigma_{a,1} = 0$ and $\sigma_{a,2} > 0$, than the fatigue life at constant stress amplitude $\sigma_{a,2}$, although it should be equal to $N(\sigma_{a,2})$ as the applied loading regime is actually a constant amplitude loading regime. The approach of Subramanyan [63] is favorable because the isodamage lines defined by Hashin and Rotem [64] become invalid at low stress amplitudes. Furthermore, the model of Subramanyan has been proven to successfully predict fatigue lives of specimens made from aluminum alloy Al-2024-T42 subjected to two-level block loading [65]. Although both models are an improvement over Miner’s rule, they have been found to be slightly non-conservative [66]. Furthermore, the model of Subramanyan [63] does not account for cycles below the fatigue limit.

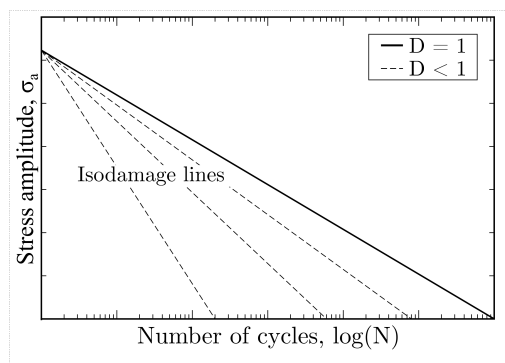


Figure 6. Isodamage line model of Hashin and Rotem [64].

El Aghoury and Galal [67] proposed a new concept called the Virtual Target Life Curve (VTLC) to alleviate some of the shortcomings of previously mentioned isodamage-based

models. They suggested that every material has a virtual (theoretically infinite) expected life that is, by definition, greater than the real failure life under constant amplitude loading. The expected life reduces as the number of cycles increases and the damage rate depends on the stress level. Overloading effects caused by stress level transitions can cause sudden damage increases. The significance of the damage increase depends on the ratio of the two stress levels. The VTLC failure criterion is reached when the accumulated number of cycles reaches the virtual target life at a certain stress level. The VTLC approach is illustrated in Figure 7. As the number of cycles increases, the slope b_v of the VLTC decreases. The VLTC rotates around the focal point (indicated in Figure 7) until it is parallel with the original S-N curve ($b_v = b$), this is when fatigue life is assumed to be exhausted.

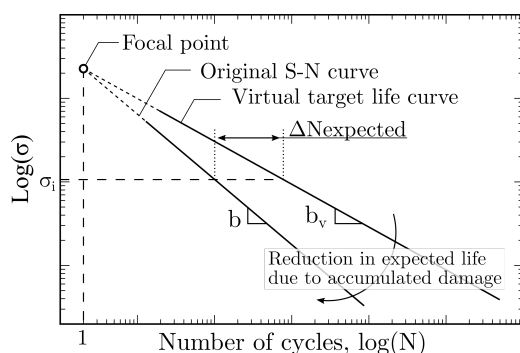


Figure 7. Graphical presentation of the virtual target life curve concept.

Rege and Pavlou [68] introduced the concept of nonlinear isodamage curves into the model of Subramanyan [63]. The concept is illustrated in Figure 8. They aimed to improve the non-conservative predictions by the models of Subramanyan [63] and Hashin and Rotem [64]. It is a one-parameter model that is easily applicable by practicing engineers. For multi-level block loading the damage up to and including load step i can be calculated using Equations (31) and (32).

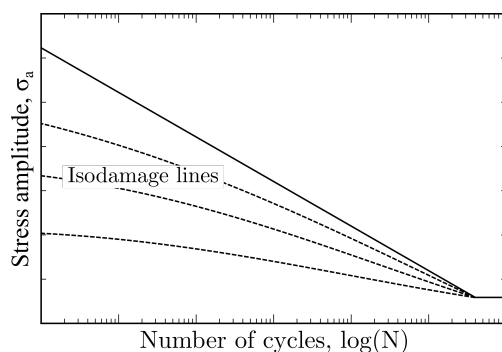


Figure 8. Nonlinear isodamage curve concept introduced by Rege and Pavlou [68].

$$\log(n_{i-1,i}) = \log(N_f) - \frac{\log(N_f) - \log(N_i)}{D_{i-1}^{1/q(\sigma_i)}} \tag{31}$$

$$D_i = \left[\frac{\tan(\theta_i)}{\tan(\theta_f)} \right]^{q(\sigma_i)} = \left[\frac{\log(N_f) - \log(N_i)}{\log(N_f) - \log(n_{i-1,i} + n_i)} \right]^{q(\sigma_i)} \tag{32}$$

N_i is the constant amplitude fatigue life at σ_i and N_f is the number of cycles at the fatigue limit. $q(\sigma_i)$ is a function of the stress amplitude for the current load step i that is best determined from experimental data but can be estimated by Equation (33). σ_s is the value of the stress amplitude where the straight S–N curve intersects the stress axis. Rege

Pavlou [70] showed that the isodamage lines can be derived from a steady state heat transfer analysis with a commercial finite element package. Therefore, the reader is referred to [70]. He compared predictions of the proposed theory with experimental results available in literature, which showed very good agreement. To use the model damage envelope principle for multi-axial fatigue, S–N curves obtained from specimens loaded under multi-axial fatigue stress should be used to derive the fatigue damage envelope. Compared to the model of Rege and Pavlou [68], Pavlou’s model [70] does not require any fitting parameters and it is valid all types of S–N curves, not only for linear ones.

Batsoulas [71] introduced the concept of hyperbolic isodamage lines. He aimed to overcome the invalidity of the straight S–N isodamage lines observed when near the axes. The hyperbolic curves satisfy the general relation:

$$\log \frac{\sigma}{\sigma'_f} = c \left(\log \frac{N}{N_e} \right)^{-1} \tag{36}$$

σ'_f is the fatigue strength coefficient and N_e is the minimum number of cycles required for damage initiation and c is a constant. The isodamage lines are defined in a $\log(\sigma/\sigma'_f)$ versus $\log(n/N_e)$ diagram where the points along the $\log(\sigma/\sigma'_f)$ versus $\log(N/N_e)$ correspond to failure. Figure 10 illustrates the hyperbolic isodamage line concept of Batsoulas [71]. A distinctive property of the proposed isodamage lines is that their points are apexes of equivalent rectangles. For example in Figure 10, the area of rectangle [OABC] is equal to the area of rectangle [OA'B'C']. Therefore, the fatigue damage corresponding to a certain isodamage line can be determined as

$$D_i = \frac{[OABC]}{[OAFE]} = \frac{\log\left(\frac{\sigma_i}{\sigma'_f}\right) \log\left(\frac{n_i}{N_e}\right)}{\log\left(\frac{\sigma_i}{\sigma'_f}\right) \log\left(\frac{N_i}{N_e}\right)} \tag{37}$$

The damage accumulation rule for multi-level loading is expressed as

$$\left(\left(\left(\frac{n_1}{N_1} \right)^{\varphi_{1,2}} + \frac{n_2}{N_2} \right)^{\varphi_{2,3}} + \dots + \frac{n_i}{N_{i-1}} \right)^{\varphi_{i-1,i}} + \frac{n_i}{N_i} = 1 \quad \text{with} \quad \varphi_{i-1,i} = \frac{\log(\sigma_{i-1}/\sigma'_f)}{\log(\sigma_i/\sigma'_f)} \tag{38}$$

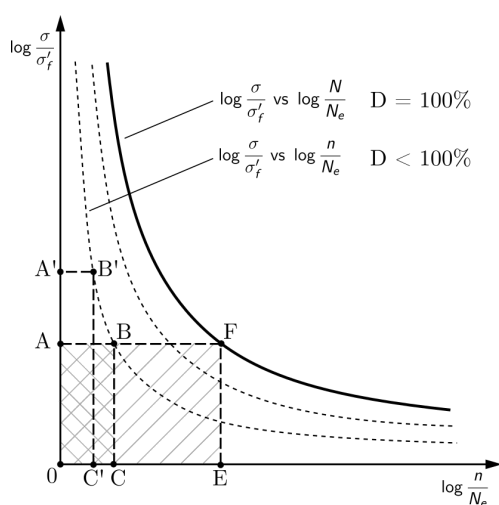


Figure 10. Hyperbolic isodamage line concept by Batsoulas [71].

A modified version of the hyperbolic isodamage curve concept was proposed by Xia et al. [72]. They combined it with the model of Ye and Wang [73] (described in Section 4.4) that is based on the exhaustion of static toughness. The modified model essentially comes down to a modification of the exponent $\varphi_{i-1,i}$ to

$$\varphi_{i-1,i} = \left(\frac{\log(\sigma_{i-1}/\sigma'_f)}{\log(\sigma_i/\sigma'_f)} \right) \left(\frac{\log N_f - \log N_i}{\log N_f - \log N_{i-1}} \right) \quad (39)$$

4. Models Based on Continuum Damage Mechanics

Continuum damage mechanics (CDM) deals with the mechanical behavior of a deteriorating medium at the continuum scale. A number of review papers have been published that provide a summary of the most important CDM based fatigue life prediction models, e.g., Fatemi and Yang [7], Krajcinovic [74], Cui [75], Silitonga et al. [76], and Santecchia et al. [16]. The foundations for CDM were laid by Kachanov [77] and Rabotnov [78]. Chaboche [79] was the first to apply CDM to fatigue life prediction. He proposed the nonlinear continuum damage (NLCD) model to describe the progressive deterioration processes before the macroscopic crack initiation. The model generalizes the NLDR model of Marco and Starkey [21] and the DCA model of Manson and Halford [26] supported by CDM. It was first described by Chaboche [79] and later reviewed by Chaboche and Lesne [80]. For uniaxial loading, the damage is expressed in Equation (40) and the number of cycles to initiation of a macroscopic crack N_F (i.e., the failure criterion) can be determined using Equation (41).

$$D = 1 - \left[1 - \left(\frac{n}{N} \right)^{\frac{1}{1-\alpha}} \right]^{\frac{1}{1+\beta}} \quad \text{with} \quad \alpha = 1 - a \left\langle \frac{\sigma_a - \sigma_{l_0}(1 - b\bar{\sigma})}{\sigma_u - \sigma_{max}} \right\rangle \quad (40)$$

$$N_F = \frac{1}{(1 + \beta)(1 - \alpha)} \left[\frac{\sigma_{max} - \bar{\sigma}}{M_0(1 - b\bar{\sigma})} \right]^{-\beta} \quad (41)$$

a , β , and M_0 are material constants; σ_{l_0} is the fatigue limit for fully reversed conditions; σ_u is the ultimate tensile strength; σ_a is the stress amplitude; and σ_{max} is the maximum stress. The symbol $\langle \cdot \rangle$ is defined as $\langle x \rangle = 0$ if $x < 0$ and $\langle x \rangle = x$ if $x > 0$. The NLCD model has some major advantages: First, it accounts for damage growth below the initial fatigue limit if the material is damaged. Second, interaction effects can be taken into account by using an additional variable to account for strain hardening. Third, the damage is explicitly dependent on the mean stress. Finally, the material parameters can easily be determined from conventional S–N curves. In order to extend the model to multi-axial loading conditions, a supplementary multi-axial fatigue criterion has to be used since the damage D is a scalar variable written in its uniaxial form. Sun et al. [81] successfully implemented the NLCD model using an effective stress in an online damage calculation framework for a steam turbine, showing its practical usability.

Since the publication of the NLCD model from Chaboche and Lesne [80], several other models based on the same theoretical considerations were developed in the field of CDM [82–87]. Fatemi and Yang [7] noted that the main differences between these models lie in the number of variables, the damage rate equation and the boundary conditions.

4.1. Models Based on the Nonlinear Continuum Damage Model of Chaboche

Throughout a number of publications [88–90], Oller et al. [91] developed a constitutive thermo-elasto-plastic-damage model that establishes a relationship between the residual material strength and the damage threshold evolution. They introduced a new state variable of fatigue $f_{red}(N, \sigma_{max}, R, \theta)$, called the reduction function, to model the nonlinear damage behaviour observed in fatigue. N is the current number of cycles, σ_{max} is the maximum applied stress, R is the stress ratio $\sigma_{min}/\sigma_{max}$, and θ is the temperature. This state variable modifies the so-called discontinuity threshold surface $F^D(S_{ij}, d)$ (yield or damage). Thus, the influence of the number of cycles is implicitly incorporated in the fatigue damage model. This approach differs from the model of Chaboche and Lesne [80] where the number of cycles is explicitly defined in the damage model. This means that fatigue phenomena can be introduced in classical constitutive damage formulations.

Dattoma et al. [92] proposed a new nonlinear uniaxial model based on the original framework of Chaboche [79]. A new expression of for the exponent α was proposed:

$$\alpha = 1 - \frac{1}{H} \left\langle \frac{\sigma_a - \sigma_f}{\sigma_u - \sigma_a} \right\rangle^a \quad (42)$$

where a and H are parameters that have to be experimentally determined. α is chosen such that it is a monotonically decreasing function of the stress to account for load interaction effects and that it is equal to 1 if the applied stress is below the fatigue limit. Dattoma et al. [92] derived that, for a multi-level loading sequence, the cumulative damage can be calculated as

$$D_i = 1 - \left[1 - \left(\frac{N_i + n_i}{N_{f_i}} \right)^{\frac{1}{1-\alpha_i}} \right]^{\frac{1}{1+\beta}} \quad (43)$$

Here, N_{f_i} is the number of cycles to failure at stress amplitude $\sigma_{a,i}$ and N_i corresponds to an equivalent number of cycles applied with stress amplitude $\sigma_{a,i}$ that causes the same amount of damage as caused by n_{i-1} cycles at $\sigma_{a,i-1}$. In the case of a load spectrum that contains several cycles below the fatigue limit, the value of α equals 1. The damage increment has to be calculated as

$$D_i = 1 - [1 - W_i]^{\frac{1}{1+\beta}} \quad (44)$$

with

$$W_i = [1 - (D_{i-1})^{1+\beta}] \exp \left[\left(\frac{n_i}{(M_0/\sigma_i)^\beta} \right) (1 + \beta) \right]$$

The CDM-based model from Dattoma et al. [92] can be used for complex, multi-level load sequences. It accounts for damage caused by cycles below the fatigue limit and all parameters can be determined from an S–N curve. The model was verified to experimental results of two-level and multi-level rotating bending experiments on 30NiCrMoV12 steel. For the multi-level loading conditions Dattoma et al. [92] considered a load history of a railway axle running onto a European line for about 3000 km. Fatigue tests were also conducted with high-to-low, low-to-high, and random loading sequences on cylindrical specimens. The model showed good agreements with experimental results. Giancane et al. [93] compared the model predictions to experiments on the same 30NiCrMoV12 steel grade for three different cylindrical specimens (one smooth and two notched specimens with different notch geometries). They concluded that the proposed CDM model is capable of satisfactory fatigue life predictions of complex geometries. They also stated that the major disadvantage of the model lies in its requirement to know the S–N curve for each considered geometry and for different load conditions.

Zhang et al. [94] proposed another modified version of the model by Chaboche and Lesne [80]. In the original model, all cycles below the fatigue limit are considered damaging once $D > 0$. It has, however, been shown that low amplitude cycles between 75% to 95% of the fatigue limit can increase the fatigue strength of the material, thus increasing the fatigue life [95–97]. Note that the low amplitude cycles still damage the material whilst also strengthening it. As such, omitting the low amplitude cycles results in an overestimation of the fatigue life while counting all those cycles results in an overly conservative estimation (e.g., NLCD model). Zhang et al. [94] introduced a strengthening function f_s to account for low amplitude cycles:

$$f_s = \begin{cases} 1 & \sigma_i \in [0, \sigma_F] \\ \exp(m'\sigma_i) & \sigma_i \in [\sigma_F, \sigma_0] \end{cases} \quad (45)$$

where m' is the strengthening coefficient related to material properties and can be obtained by test, and σ_F is the lower limit of the strengthening stress. The damage can then

be calculated by multiplying Equation (40) with the strengthening function defined in Equation (45). To determine if the low amplitude cycles cause damage or induce strengthening, Zhang et al. [94] additionally introduced the use of a membership function based on fuzzy logic mathematics. The model was validated to experimental data of multi-level loading including low amplitude cycles below the fatigue limit. They found that the new model performs better than the NLCD with relative errors between 14.96% to 21.5% for Chaboche's model and 2.5% to 8.38% for the proposed model.

4.2. Models Based on Thermo-Mechanical Principles

Bhattacharya and Ellingwood [98] argued that the then available approaches introduce unknown material constants in damage growth quantification which makes their applicability difficult or even impossible. They also argued that thermodynamics-based CDM models of damage growth lack continuity with the first principles of thermodynamics and mechanics and provided an extensive overview of these models and their deficiencies in [98]. In order to overcome this deficiency, they proposed a new thermodynamic framework for a CDM-based approach to structural deterioration [98,99]. Based on the first principles of thermodynamics, a coupled set of partial differential equations for damage growth in deformable bodies was obtained. Under the assumption of uniaxial loading and isotropic damage growth, a closed-form solution for fatigue damage could be derived from the differential equations. For strain-controlled loading, the fatigue damage after n cycles is expressed as

$$D_n = 1 - (1 - D_0) \left(\frac{\frac{1}{1+\frac{1}{M'}} \Delta \varepsilon_{p0}^{1+(1/M')} - \Delta \varepsilon_{p1}^{1/M'} \Delta \varepsilon_{p0} + C}{\frac{1}{1+\frac{1}{M'}} \Delta \varepsilon_p^{1+(1/M')} - \Delta \varepsilon_{p1}^{1/M'} \Delta \varepsilon_p + C} \right)^n \quad (46)$$

Here, D_0 is the initial damage, M' is the cyclic hardening exponent, $\Delta \varepsilon_p$ is the plastic strain range, and $\Delta \varepsilon_{p0}$ is the threshold plastic strain range. ε_{p1} is the plastic strain range corresponding to the strain where the reloading curve cuts the monotonic strain-axis. Using Equation (46), it is possible to determine the number of cycles to crack initiation using the conditions given in Equation (47) if the critical damage D_c is known. N_I is the number of cycles to macroscopic crack initiation (localization).

$$\begin{cases} D_{N_I-1} < D_c \\ D_{N_I} \geq D_c \end{cases} \quad (47)$$

Li et al. [100] proposed a damage model based on the accumulation of micro-plastic strain (macro-plastic strain is assumed to be zero), the strain energy density release rate and the current state of damage. The model was specifically developed to evaluate the damage accumulation in bridges under traffic loading. They started from a general constitutive model developed by Lemaitre [101]. The model expresses the fatigue damage rate for high-cycle fatigue damage and is given in Equation (48).

$$\dot{D} = \frac{R_v \sigma_{eq}^2 |\sigma_{eq} - \bar{\sigma}_{eq}|^\beta}{B(1-D)^\alpha} \langle \dot{\sigma}_{eq} \rangle \quad (48)$$

σ_{eq} is the von Mises equivalent stress and R_v is a triaxiality function that models the influence of the triaxiality ratio (σ_H/σ_{eq} with σ_H the hydrostatic stress) on damage and rupture. α determines the nonlinearity of the damage function and is a function of the stress range. The damage rate $\dot{D} = 0$ if $\sigma^* < \sigma_f$ with σ_f the fatigue limit. σ^* is defined as the damage equivalent stress and was defined by Lemaitre [101] as the stress which for damage acts as the von Mises stress does for plasticity. From Equation (48), Li et al. [100] derived the following damage model,

$$D_{i+1} = 1 - \left\{ (1 - D_i)^{\alpha_1+1} - \frac{(\alpha_1 + 1) N_{bl}^i}{B(\beta + 3)} \sum_{j=1}^{m_{rb}} [(\sigma_j + 2\sigma_{mj}) \sigma_j]^{\frac{\beta+3}{2}} (1 - D_i)^{\alpha_1 - \alpha_j} \right\}^{\frac{1}{\alpha_1+1}} \quad (49)$$

with

$$\alpha_i = k_\alpha \sigma_i + \alpha_0 \quad (50)$$

$B, \beta, k_\alpha,$ and α_0 are material parameters that can be determined from the S–N curve. m_{rb} is the number of cycles with the maximum stress in the representative block larger than the fatigue limit, N_{bl} the number of loading blocks, σ_j and σ_{mj} are the stress range and mean stress for the j th cycle, respectively. The damage model has been presented and successfully applied for fatigue damage assessment of the Tsing Ma Bridge under various loading conditions in a number of papers [100,102–106]. Equation (48) has been used as the basis for other cumulative damage models intended for fatigue damage assessment of long span bridges by other researchers as well, e.g., [107,108]. These models are very similar to (49) and will therefore not be discussed in detail.

4.3. Models Based on the Damage Stress Concept

Mesmacque et al. [109] proposed the CDM-based damage stress model (DSM). The DSM is based on the hypothesis that if the physical state of damage does not change, the fatigue life depends only on the loading conditions. The residual fatigue life of a structure loaded for n_i cycles with a stress amplitude σ_i , equals to $N_{iR} = N_i - n_i$. The residual life corresponds to an admissible stress level $\sigma_{ed,i}$ on the S–N curve, this is illustrated in Figure 11. The stress $\sigma_{ed,i}$ is called the damage stress after n_i cycles of loading. In other words, the damage stress is defined as the stress corresponding to the instantaneous residual life on the S–N curve.

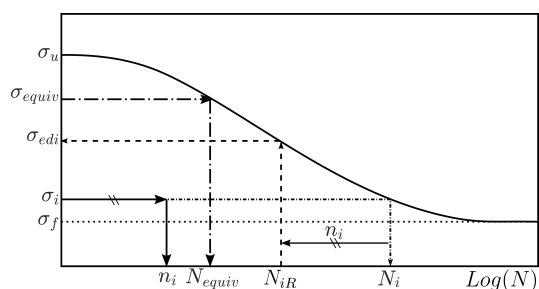


Figure 11. Illustration of the parameters introduced by the damage stress model [109].

A new expression for the damage parameter D_i is introduced and defined as

$$D_i = \frac{\sigma_{ed,i} - \sigma_i}{\sigma_u - \sigma_i} \quad (51)$$

here σ_u is the ultimate stress. For multi-level loading, the damage can be transferred to level $i + 1$ using Equation (52). It is then possible to calculate the number of cycles N_{equiv} (see Figure 11) at level $i + 1$ equivalent to n_i cycles at level i . The residual lifetime after n_{i+1} load cycles with amplitude σ_{i+1} is then $N_{i+1} - n_{i+1}$. The equivalent damage stress σ_{equiv} at level $i + 1$ can be calculated using Equation (52). Initially, when $D = 0$, the damage stress $\sigma_{ed} = \sigma_i$. Failure occurs when $D = 1$, which is when the damage stress $\sigma_{ed} = \sigma_u$.

$$D_i = \frac{\sigma_{ed,i} - \sigma_i}{\sigma_u - \sigma_i} = \frac{\sigma_{equiv} - \sigma_{i+1}}{\sigma_u - \sigma_{i+1}} \quad (52)$$

Mesmacque et al. [109] compared the model with Miner’s rule for two-level and four-level block loading sequences. For the former, differences between the experimental values and the results of the DSM model varied from 7.7% to 89% and for Miner’s rule from 16.8% to 155%. For the latter, differences between the experimental values and the results of the DSM model varied from 2.5% to 6.5% and for Miner’s rule from 4.7% to

75.1%. The model was further compared to Miner's rule by Aid et al. [110] for multi-level block sequences and a random loading sequence on both aluminum and steel alloys. The general conclusion was similar, i.e., that fatigue lives estimated with the DSM deviate significantly less from the experimentally obtained values compared to estimations based on Miner's rule. Siriwardane et al. [111] used the DSM for fatigue life prediction of riveted railway bridges. Both uniaxial and multi-axial fatigue were considered. A difference of 10 to 15 years between lifetimes estimated with Miner's rule and the DSM were found. Siriwardane et al. [111] advised to use the DSM if stress histories are known. Adasooriya and Siriwardane [112] extended the study of Siriwardane et al. [111] to fatigue life estimation of corroded bridge members. They proposed a method that consists of the stress history, a full range S–N curve that represents the corrosive environment and the DSM to predict fatigue life of corroded structures. They concluded that the proposed method is suitable for the fatigue assessment of structures subjected to uniform corrosion. Aeran et al. [42] also compared predictions from the DSM to two-level block loading experiments on C45 and 16Mn steel, again finding good agreement with the experimental results. Rege and Pavlou [68] reported that the DSM showed poor performance when the S–N curve is linear in a semi-log plot while the model was originally only verified for S–N curves that are linear in a log-log diagram.

Aid et al. [113] proposed an extension of the DSM, initially developed for uniaxial loading, to bi-axial random loading applied to cruciform specimens. For the application of the DSM towards multi-axial fatigue, an equivalent stress criterion has to be used. Aid et al. [113] compared the DSM model coupled with the von Mises (DSM-VM) [114], Sines (DSM-SI) [115] and Crossland (DSM-CR) [116] criteria. The extended DSM model was also compared to other models developed for multi-axial fatigue conditions: the Smith–Watson–Topper damage parameter used by Bannantine and Socie [117], Fatemi–Socie [118], Socie for high-cycle fatigue [119], Wang–Brown [120], and Lagoda–Macha [121]. The methods of Fatemi–Socie, Socie, and the DSM-VM were shown to produce overly conservative results. Both the DSM-CR and DSM-SI produced satisfying results. Finally, they recommended the DSM-SI model due to the lowest average deviation of the lifetime predictions with respect to the experimental results. Benkabouche et al. [122] developed a numerical tool using Matlab and finite elements for fatigue damage accumulation using the DSM-CR.

Although these extended DSM model predictions agree well with experimental data, it requires three S–N curves $\sigma_{-1}(N)$, $\tau_{-1}(N)$ and $\sigma_0(N)$, which correspond to uniaxial reversed bending ($R = -1$), reversed torsion ($R = -1$) and uni-axial repeated bending ($R = 0$), respectively. This makes the engineering applicability limited as these types of S–N curves are very scarce. Shen et al. [123] proposed the use of two additional relations, Equation (53) proposed in the work of Robert [124] and Equation (54) known as Gerber's parabola such that a single S–N curve is enough.

$$\frac{\tau_{-1}(N)}{\sigma_{-1}(N)} = 0.56 \quad (53)$$

$$\frac{\sigma_a}{\sigma_{-1}} \left(\frac{\sigma_m}{\sigma_u} \right)^2 = 1 \quad (54)$$

Shen et al. [123] then proposed a similar extension of the DSM with Sines criterion (DSM-S) [115], the Dang Van criterion (DSM-DV) [125], and Robert's criterion (DSM-RB) [126]. The models were compared to bi-axial fatigue experiments on 6082-T6 aluminium cruciform specimens. Shen et al. [123] performed constant amplitude, two-level block loading, three-level block loading, and two-level repeated block loading experiments. They concluded that the DSM-RB provided the best results and that the DSM-SI and DSM-DV resulted in unrealistic values (residual lifetime smaller than zero) in a number of cases. Do take note however that the DSM-RB model predictions had significantly larger

relative errors in most cases. A clear summary with quantifiable performance parameters is missing.

4.4. Material Degradation-Based Models

A number of experimental studies [127,128] have shown that static mechanical properties (Young's modulus E , yield stress $\sigma_{0.2}$, ultimate tensile strength σ_{UTS} , etc.) of virgin material differ from post-fatigue static properties. This material degradation as a function of the cycle ratio n/N has been used to develop fatigue damage accumulation models.

In 2001, Ye and Wang [73] proposed a new damage accumulation model based on the exhaustion of static toughness and dissipation of cyclic plastic strain energy during fatigue. Based on experimental data from the work in [127], it was concluded that, as the material is progressively exposed to more fatigue cycles, its ability to absorb energy (i.e., the static toughness) decreases. In other words, the internal energy of the material increases which results in material damage such as formation of internal defects (voids and cracks), translation of dislocations, phase changes, and development of residual stress. Considering the aforementioned, Ye and Wang [73] expressed the damage as irreversible dissipation of cyclic plastic strain energy that results in fatigue fracture when a critical value is reached. The scalar damage value D is expressed as

$$D_i = -\frac{D_{N_f-1}}{\ln N_i} \ln \left(1 - \frac{n_i}{N_i} \right) \quad \text{with} \quad D_{N_i-1} = 1 - \frac{\sigma_a^2}{2EU_{T0}} \quad (55)$$

Here, E is Young's modulus, U_{T0} is the static toughness of the material in its virgin state, σ_a is the stress amplitude, and n_i and N_i have their usual meaning. D_{N_f-1} is the critical value of the damage variable.

Lv et al. [129] proposed a modified version of the damage model by Ye and Wang [73]. Inspired by the works of Corten and Dolan [30] and Morrow [130], they introduced a load interaction factor in Equation (55) to account for load sequence effects. Equation (55) becomes

$$D = -\frac{D_{N_f-1}}{\ln(N_i)} \ln \left(1 - \frac{n_i}{N_i} \right) \left(\frac{\sigma_i}{\sigma_{max}} \right) \quad (56)$$

Assuming that $D_{N_f-i}/D_{N_f-(i-1)} \approx 1$, which is a reasonable assumption for high-cycle fatigue, the number of cycles to failure for multi-level block loading can be calculated using Equation (57). Omitting the interaction factor in the exponents reduces Equation (57) to the original model of Ye and Wang [73].

$$D = \frac{n_i}{N_i} + \left[\left[\left(\frac{n_1}{N_1} \right)^{\frac{\ln(N_2)}{\ln(N_1)} \frac{\sigma_1}{\sigma_2}} + \frac{n_2}{N_2} \right]^{\frac{\ln(N_3)}{\ln(N_2)} \frac{\sigma_2}{\sigma_3}} + \dots + \frac{n_{i-1}}{N_{i+1}} \right]^{\frac{\ln(N_i)}{\ln(N_{i-1})} \frac{\sigma_{i-1}}{\sigma_i}} = 1 \quad (57)$$

Lv et al. [129] used data from two-level block loading experiments on smooth and notched specimens of C45 and 16Mn steel to verify their modified damage accumulation model. Through the addition of an interaction factor, the predictions of the original model were indeed improved, indicating that load interaction effects should not be ignored.

A different type of material degradation approach was proposed by Böhm et al. [131,132]. They defined a fatigue damage accumulation model based on theoretical assumptions taken from the field of psychology. The Ebbinghaus forgetting curve is an exponential function that describes the decline of memory retention in time when a person makes no attempt to retain it. In order to describe the material degradation due to fatigue, the time function had to be converted to a function of the number of cycles. Material memory was defined as

$$m = (a - c)^e - \frac{N_f}{d} + c \quad (58)$$

m is the material memory performance of the material, a is the memorization rate, d is the reciprocal value of the forgetting rate given in number of cycles, and c is the horizontal asymptote of the function. Using the new material memory concept described by Equation (58), Böhm et al. [131,132] derived the damage accumulation function given in Equation (59). The reader is referred to [131] for the full derivation. $N_f = \sum_i n_i$ is the total number of cycles to failure, n_i and N_i have their usual meaning.

$$D = \sum_{i=1}^j \frac{N_f - e^{-\frac{n_i}{d}}}{d \left(1 - e^{-\frac{N_f}{d}}\right) N_i} \quad (59)$$

Peng et al. [55] combined the material memory concept with a residual S–N curve approach. Conventionally, the residual S–N curve describes the residual life of the material or component after it has been stressed with a number of cycles. The residual S–N curve then has the same slope as the S–N curve of the virgin material but a different S-intercept. Peng et al. [55] considered the slope of the residual S–N curve Δb as a variable that depends on the loading history. Initially the slope of the residual S–N curve is the same as the S–N curve of the virgin material b , but as the fatigue damage increases the slope Δb does too. The slope ratio $b/\Delta b$ is hypothesized to represent fatigue damage accumulation. Based on the material memory degradation concept, a decay coefficient α is defined which relates to the slope ratio $b/\Delta b$. The memory degradation concept is thus used to model the changes of the residual S–N curve. For the i_{th} loading block this leads to

$$b/\Delta b = \alpha_i = \frac{e^{-\frac{n_i}{N_i}} - e^{-1}}{1 - e^{-1}} \quad (60)$$

Using the relation defined in Equation (60), Peng et al. [55] derived a new cumulative fatigue damage rule:

$$D = \sum_1^i \frac{n_i}{N_i} \times \prod_{j=1}^{i-1} \left(\frac{N_i}{N_{i+1}}\right) \left(\prod_{k=1}^j \frac{e^{-\frac{n_k}{N_k}} - e^{-1}}{1 - e^{-1}}\right)^{-1} \quad (61)$$

The results obtained using this damage model were compared to results obtained with Miner's rule, the model in [30] and the model of Kwofie and Rahbar [39] for two-level and multi-level block loading. It was concluded that the proposed model performs better than its counterparts because the scalar damage variable is more sensitive to load level changes.

Zhou et al. [133] also proposed a cumulative fatigue damage model based on the material memory concept of [131]. The damage model is defined as

$$D_i = \left(\frac{1 - e^{-\frac{n_i}{N_i}}}{1 - e^{-1}}\right)^{\zeta(\sqrt{\sigma_{max,i}} \sigma_{a,i})^\delta} \quad (62)$$

δ and ζ are fitting parameters. Zhou et al. [133] proposed a value $\delta = -5.78$ based on a fit to 18 two-level block loading experiments on 30NiCrMoV12 steel [92]. They completely omitted ζ when calculating the residual life. Unfortunately, no reasoning is provided for this. They also assumed that $\delta = -5.78$ can be used for all metals used in their study. Model estimations with these parameter values were compared to four different experiments and three damage models, i.e., Miner's rule, the model of Lv et al. [129] and the model of Kwofie and Rahbar [39]. They reported that lifetime estimations obtained with the proposed model showed less deviation than the estimations obtained with the other models. The difference in performance with the model of Lv et al. [129] is however rather limited. Furthermore, because the model proposed by Zhou et al. [133] depends on fitted parameters, it is less generalized. Moreover, the lack of explanation why the parameter ζ can simply be dropped

and the extremely small dataset used to determine δ do not allow to generalize the use of this model at this stage.

4.5. Energy-Based Rules

Strain energy density-based damage rules for high-cycle fatigue originate from the observation that the plastic energy dissipation ΔW^p during cyclic loading could be used as criterion for low-cycle fatigue failure [134,135]. This method is however limited to low-cycle fatigue because, as the magnitude of the strain range $\Delta\varepsilon$ decreases, the plastic component $\Delta\varepsilon^p \rightarrow 0$, and thus the plastic strain energy density $\Delta W^p \rightarrow 0$. Ellyin and co-workers [136–138] proposed a new criterion, termed the total strain energy density ΔW^t , that combines the damaging plastic strain energy density ΔW^p and the elastic strain energy associated with the tensile mode ΔW^{e+} that facilitates crack growth [139]. Thereby they developed a unified approach for low and high-cycle fatigue. The fatigue life is a function of the total energy input, and is described by a power law relation that is represented by a linear curve in a double logarithmic plot, similar to the S–N curve and is shown in Figure 12. The power law has the following form.

$$\Delta W^t = \Delta W^{e+} + \Delta W^p = \kappa N^\alpha + C \tag{63}$$

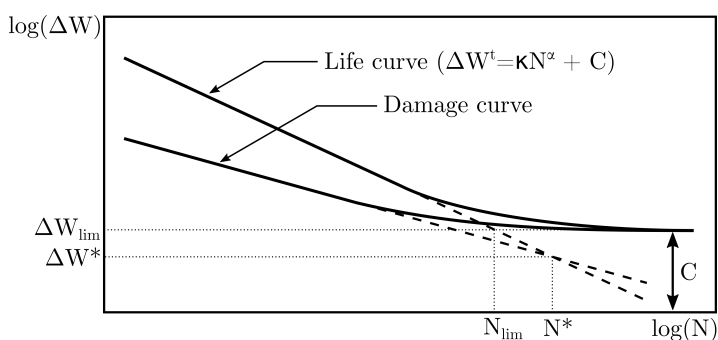


Figure 12. Critical damage and life curves intersecting at the reduced fatigue limit.

κ , α , and C are material parameters. The constant C is the portion of the tensile mode elastic energy input and is related to the material fatigue limit strain energy density ΔW_{lim} . Golos and Ellyin [139] also established a critical damage curve (illustrated in Figure 12) in terms of the total strain energy density that represents the transition between crack initiation and the subsequent crack propagation phase. Golos and Ellyin [137] developed a fatigue criterion that can be used to determine the fatigue life in a multi-block loading. The residual life in the i_{th} load block can be determined as

$$\left\{ \left[\left(\frac{n_1}{N_1} \right)^{\frac{\log\left(\frac{N_2}{N^*}\right)}{\log\left(\frac{N_1}{N^*}\right)} + \frac{n_2}{N_2} \right]^{\frac{\log\left(\frac{N_2}{N^*}\right)}{\log\left(\frac{N_2}{N^*}\right)}} + \dots + \frac{n_{i-1}}{N_{i-1}} \right\}^{\frac{\log\left(\frac{N_i}{N^*}\right)}{\log\left(\frac{N_{i-1}}{N^*}\right)}} + \frac{n_i}{N_i} = 1 \tag{64}$$

$\Delta W^* < \Delta W_{lim}$ and its value can be obtained from the intersection of the extrapolated $\Delta W - N_f$ curve with the critical damage curve as shown in Figure 12. The value of N^* corresponds to ΔW^* on the N axis of the $\Delta W - N_f$ life curve and is referred to as the reduced fatigue limit.

Park et al. [140] proposed a modified version of the strain energy density model in Equation (63) to describe the fatigue behavior of an anisotropic rolled AZ31 magnesium alloy. Hereto, they included a term that accounts for the plastic strain energy consumed by

the mean strain; this is shown in Equation (65). $f(\varepsilon_m)$ is the plastic strain energy associated with the mean strain and γ is a material constant. Their model showed a good agreement with the experimental data.

$$\Delta W^t = \Delta W^{e+} + \Delta W^p + \left\{ \frac{f(\varepsilon_m)}{N_f} \right\}^\gamma = \kappa N^\alpha + C \quad (65)$$

Ellyin and Golos [141] extended the total strain energy density to multi-axial conditions under (nearly) proportional fatigue loading. A review of energy-based multi-axial fatigue failure criteria was published by Macha and Sonsino [142]. They concluded that criteria which include the strain energy density in the fracture plane or critical plane are the most promising.

Lagoda et al. [121] showed that the normal strain energy density in the critical plane is an efficient parameter for high-cycle fatigue life prediction under random and cyclic non-proportional loading. They also proposed a new strain energy density parameter that allows to distinguish between positive strain energy density occurring in a tension path and negative strain energy density occurring in the compression path. Whereas previous approaches only considered the amplitudes of stresses, strains, and the dissipated energy, the proposed strain energy density parameter also accounts for the history of the considered parameter. The parameter was implemented in a fatigue life calculation algorithm which was validated to a number of experimental studies on steels and cast irons [143,144].

Jahed and Varvani-Farahani [145] proposed an energy-based fatigue life prediction model for metallic components. The model estimates upper and lower bounds for experimental fatigue lives. The model was initially developed for tension, torsion and proportional multi-axial loading conditions. The number of cycles to failure N_F may be determined as

$$N_F = \frac{\Delta E_A}{\Delta E} N_A + \frac{\Delta E_T}{\Delta E} N_T \quad (66)$$

ΔE_A and ΔE_T are the energy due to a purely tensile loading and the energy due to a purely torsion loading, respectively. ΔE is the total elastic–plastic energy. It was later extended to non-proportional loading [146]. The method in [145,146] was used by Gu et al. [147] for fatigue life prediction of a mining truck welded frame achieving good agreement with experimental observations.

Scott-Emuakpor et al. [148–152] performed fully reversed axial tension–compression tests and rotating bending tests for 6061-T6 aluminium. They observed that the experimental fatigue lives are approximately 20% higher for the rotating bending tests than for tension–compression test. This was attributed to the gradient effect of the normal stress [153]. Over a number of works they proposed and extended a uniaxial, energy-based criteria for high-cycle tension–compression fatigue that accounts for the mean stress, and for high-cycle bending fatigue that accounts for the gradient effect and mean stress effects. The model is based on the assumption that the strain energy required to fracture a material in monotonic loading is the same as the strain energy required to cause fatigue failure, i.e., during cyclic loading, hysteresis energy gradually builds up in each cycle until the accumulated amount is equal to the fracture energy determined from a static test [154]. The energy required for fracture is calculated as

$$W_f = \sigma_f \left(\varepsilon - \frac{\sigma_f}{2E} \right) - \sigma_o \varepsilon_o \left(\cosh \frac{\sigma_f}{\sigma_o} - 1 \right) \quad (67)$$

σ_f and ε_f are the true stress and strain at fracture, respectively. ε_o is a curve fit parameter and σ_o is estimated as

$$\sigma_o = \frac{\sigma_f - \sigma_y}{\ln \left(\frac{\varepsilon_f}{0.002} \right)} \quad (68)$$

where σ_f is the true stress at fracture, ε_f is the true fracture strain, and σ_y is the yield stress. Model estimations have been compared to experimental results on Al 6061-T6 and Ti 6Al-4V specimens, giving good agreement. Scott-Emuakpor et al. [155] extended the model to multi-axial and transverse shear loading.

The model of Scott-Emuakpor et al. [155] is based on the assumption that the strain energy density is the same for each cycle, which is considered to be an oversimplification [156]. It has been observed for axial and torsional shear loading that the strain energy density decreases slightly from the constant level at around 90% of the expected fatigue life, and then the energy increases rapidly until fracture [157,158]. Letcher et al. [159] defined a new material property named the “critical lifetime” which occurs when the steady-state value of the cyclic strain energy density deviates by 5%. The critical lifetime concept was included in the strain energy density model of Scott-Emuakpor et al. [155] such that conservative lifetime estimations are obtained in an intelligent manner.

Djebli et al. [160] proposed an energy-based version of the DSM by Mesmacque et al. [109] discussed in Section 4.3. They introduced a new damage parameter D_i , defined as

$$D_i = \frac{W_{ed,i} - W_i}{W_u - W_i} \quad (69)$$

$W_{ed,i}$ is the energy due to the damage stress, W_i is the energy due to the applied stress, and W_u is the energy corresponding to the ultimate stress of the material. The fatigue lifetime calculation is similar to the original DSM model. Instead of using an S–N life curve, the curve is rescaled to a W–N curve. In the case of high-cycle fatigue, it can be modeled by the Basquin function $W = \kappa N^\alpha$. When the characteristic $(\sigma_a - N)$ is used, the axis σ_a should be replaced by W_a , where $W_a = \sigma_a / (2E)$ [121].

Peng et al. [161] proposed a new approach, named the fatigue driving energy (FDE) approach. The FDE is a combination of the FDS approach proposed by Kwofie and Rahbar [39] and the strain energy density (SED). The aim of the proposed model is to overcome several deficiencies identified in the original FDS model. Assume a two-level low-to-high block loading sequence where the consumed life fraction by the first block is minimal. Determining an equivalent fatigue driving stress for the second, higher stress, load block would be impossible. Furthermore, an equivalent fatigue driving stress does not necessarily correspond to equivalent damage. Peng et al. [161] proposed a new fatigue damage accumulation model defined as

$$D = \frac{W_D - W_{D_0}}{W_{D_c} - W_{D_0}} = \frac{N^{-2b} \frac{n}{N} - 1}{N^{-2b} - 1} \quad (70)$$

with

$$W_D = \frac{1}{2E} \sigma^2 N^{-\frac{2bm}{N}} \Rightarrow \begin{cases} W_{D_0} = \frac{\sigma^2}{2E}, & \frac{n}{N} = 0 \\ W_{D_c} = \frac{A^2}{2E}, & \frac{n}{N} = 1 \end{cases} \quad (71)$$

where W is the SED, W_D is the FDE, W_{D_0} is the SED for the initial state without damage, W_{D_c} is the critical SED (i.e., $D = 1$), and A and b are the material constant and exponent of the Basquin equation, respectively. The damage accumulation model in Equation (70) was modified to account for load interactions by the addition of a load interaction factor. It can be shown that the residual lifetime for multi-level block loading can be estimated as

$$\frac{n_i}{N_i} = 1 - \frac{1}{-2b \ln(N_i)} \ln \left(\left(N_i^{-2b} - 1 \right) \left(\frac{N_{i-1}^{-2b} \left[\frac{n_{i-1}}{N_{i-1}} + 1 - \frac{n_{i-1}}{N_{i-1}} \right] - 1}{N_{i-1}^{-2b} - 1} \right)^{\frac{\sigma_{i-2}}{\sigma_{i-1}} \times \frac{\sigma_{i-2}}{\sigma_{i-1}}} + 1 \right) \quad (72)$$

Peng et al. [161] used five experimental datasets for different geometries to compare lifetime estimations of the proposed model (both with and without taking load interaction

into account) to estimations of Miner's rule. Compared to Miner's rule, the proposed model based on FDE provided more accurate lifetime estimations.

5. Conclusions

A review of cumulative damage and life prediction models for high-cycle fatigue has been presented. The article focused on models published after 1998, as a follow-up to the famous review article of Fatemi and Yang [7]. The authors do not claim that this review is exhaustive, but it does provide a comprehensive overview of the state-of-the-art.

It is evident from the previous sections that a very large number of fatigue damage accumulation models is available in literature and that more are being published each year. What is remarkable is that the new models always seem to outperform the models that they are compared to. Note, however, that there are almost no independent studies to be found that compare different fatigue damage accumulation models to various independent datasets. Furthermore, most fatigue damage models available have only been validated to relatively small experimental datasets which makes it impossible to judge their generic performance. A similar concern was raised by Patil et al. [162], who pointed out that a significant number of cumulative fatigue damage models have been developed based on particular datasets. A significant number of nonlinear cumulative damage models are based on the observations that high-low loading is more damaging than low-high loading and that for high-low loading Miners rule is not conservative. However, Taheri and co-workers [163–166] have shown that this is not the case for all metals which invalidates a lot of damage models for these types of metals. Thus, although numerous nonlinear damage models are often capable of producing satisfying results for a specific set of experiments, Miner's rule still remains the most widely used for fatigue design under variable amplitude loading.

Although more than 20 years have passed since the comprehensive review of Fatemi and Yang [7], the conclusions remain largely the same. Fatigue damage accumulation is a complex process which means that the development of an all encompassing, generalized model is extremely difficult. Based on the current state-of-the-art, there should be an increased focus on verification and comparison of existing models to a wide range of experimental datasets. In an effort to aid this goal, a collection of the various available raw datasets published in literature would be a valuable document. Furthermore, experimental data is often reported in graphic form only (e.g., S–N curves) which hinders use by other researchers, as such the addition of tabulated data in, for example, an appendix is essential for the collaborative research effort.

Funding: This research was funded by VLAIO project number 179P04718W.

Acknowledgments: The authors acknowledge the support of SIM (Strategic Initiative Materials in Flanders) and IBN Offshore Energy.

Conflicts of Interest: The authors declare no conflict of interest. The funders had no role in the design of the study; in the collection, analyses, or interpretation of data; in the writing of the manuscript; or in the decision to publish the results.

References

1. Palmgren, A. Durability of ball bearings. *ZVDI* **1924**, *68*, 339–341.
2. Miner, M.A. Cumulative damage in Fatigue. *J. Appl. Mech.* **1945**, *12*, A159–A164.
3. Eurocode 3. *Eurocode 3: Design of steel structures—Part 1–9: Fatigue*; Technical Report; European Committee for Standardisation: Brussels, Belgium, 2005.
4. DNV. *DNVGL-RP-C203: Fatigue Design of Offshore Structures*; Technical Report April 2016; DNV GL: Oslo, Norway, 2016.
5. British Standards Institution. *BSI Standards Publication Guide to Fatigue Design and Assessment of Steel Products*; Technical Report; The British Standards Institution: London, UK, 2014.
6. Schütz, W. A history of fatigue. *Eng. Fract. Mech.* **1996**, *54*, 263–300. [[CrossRef](#)]
7. Fatemi, A.; Yang, L. Cumulative fatigue damage and life prediction theories: A survey of the state of the art for homogeneous materials. *Int. J. Fatigue* **1998**, *20*, 9–34. [[CrossRef](#)]
8. Schijve, J. *Fatigue of Structures and Materials*, 2nd ed.; Springer: Delft, The Netherlands, 2008; p. 627.

9. Haibach, E. The allowable stresses under variable amplitude loading of welded joints. In *Proceedings of the Conference of the Fatigue Welded Structures*; The Welding Institute: Cambridgeshire South East, UK, 1971; Volume 2, pp. 328–339.
10. Sonsino, C.M.; Łagoda, T.; Demofonti, G. Damage accumulation under variable amplitude loading of welded medium- and high-strength steels. *Int. J. Fatigue* **2004**, *26*, 487–495. [[CrossRef](#)]
11. Sonsino, C.M. Fatigue testing under variable amplitude loading. *Int. J. Fatigue* **2007**, *29*, 1080–1089. [[CrossRef](#)]
12. Schoenborn, S.; Kaufmann, H.; Sonsino, C.M.; Heim, R. Cumulative damage of high-strength cast iron alloys for automotive applications. *Procedia Eng.* **2015**, *101*, 440–449. [[CrossRef](#)]
13. He, L.; Akebono, H.; Sugeta, A.; Hayashi, Y. Cumulative fatigue damage of stress below the fatigue limit in weldment steel under block loading. *Fatigue Fract. Eng. Mater. Struct.* **2020**, *43*, 1419–1432. [[CrossRef](#)]
14. Liu, M.D.; Xiong, J.J.; Wang, C.Q. A modified accumulation damage algorithm for predicting corrosion fatigue life by considering load interaction for aluminum alloys. *Int. J. Damage Mech.* **2018**, *28*, 270–290. [[CrossRef](#)]
15. Chang, J.; Szamossi, M.; Liu, K. Random spectrum fatigue crack life predictions with or without considering load interactions. In *Methods and Models for Predicting Fatigue Crack Growth under Random Loading*; ASTM International: West Conshohocken, PA, USA, 1981.
16. Santecchia, E.; Hamouda, A.M.S.; Musharavati, F.; Zalnezhad, E.; Cabibbo, M.; El Mehtedi, M.; Spigarelli, S. A Review on Fatigue Life Prediction Methods for Metals. *Adv. Mater. Sci. Eng.* **2016**, *2016*, 9573524. [[CrossRef](#)]
17. Bandara, C.S.; Siriwardane, S.C.; Dissanayake, U.I.; Dissanayake, R. Fatigue failure predictions for steels in the very high cycle region—A review and recommendations. *Eng. Fail. Anal.* **2014**, *45*, 421–435. [[CrossRef](#)]
18. Jimenez-Martinez, M. Fatigue of offshore structures: A review of statistical fatigue damage assessment for stochastic loadings. *Int. J. Fatigue* **2020**, *132*. [[CrossRef](#)]
19. Zhu, S.P.; Huang, H.Z.; Liu, Y.; He, L.P.; Liao, Q. A practical method for determining the Corten-Dolan exponent and its application to fatigue life prediction. *Int. J. Turbo JET Engines* **2012**, *29*, 79–87. [[CrossRef](#)]
20. Richart, F.E.; Newmark, N.M. An hypothesis for the determination of cumulative damage in fatigue. In *Civil Engineering Classics*; Newmark, N.M., Ed.; ASCE: Reston, VA, USA, 1948; pp. 279–312.
21. Marco, S.M.; Starkey, W.L. A concept of fatigue damage. *Trans. ASME* **1954**, *76*, 627–632.
22. Langer, B.F. Fatigue failure from stress cycles of varying amplitude. *J. Appl. Mech.* **1937**, *59*, A160–A162.
23. Grover, H. An observation concerning the cycle ratio in cumulative damage. In *Symposium on Fatigue of Aircraft Structures*; ASTM International: West Conshohocken, PA, USA, 1960.
24. Manson, S. Interfaces between creep, fracture and fatigue. *Int. J. Fract. Mech.* **1966**, *2*, 328–363. [[CrossRef](#)]
25. Manson, S.; Freche, J.; Ensign, C. *Application of a Double Linear Damage Rule to Cumulative Fatigue Damage*; Technical Report; Manson: West Conshohocken, PA, USA, 1967.
26. Manson, S.S.; Halford, G.R. Practical implementation of the double linear damage rule and damage curve approach for treating cumulative fatigue damage. *Int. J. Fract.* **1981**, *17*, 169–192. [[CrossRef](#)]
27. Costa, J.D.; Ferreira, J.A.; Borrego, L.P.; Abreu, L.P. Fatigue behaviour of AA6082 friction stir welds under variable loadings. *Int. J. Fatigue* **2012**, *37*, 8–16. [[CrossRef](#)]
28. Inoma, J.E.; Pavlou, D.G.; Zec, J. Implementation of linear, double-linear, and nonlinear fatigue damage accumulation rules for fatigue life prediction of offshore drilling top-drive tie-rods. In *IOP Conference Series: Materials Science and Engineering*; Institute of Physics Publishing: Bristol, UK, 2019; Volume 700. [[CrossRef](#)]
29. Manson, S.; Halford, G. Re-examination of cumulative fatigue damage analysis—An engineering perspective. *Eng. Fract. Mech.* **1986**, *25*, 539–571. [[CrossRef](#)]
30. Corten, H.T.; Dolan, T.J. Cumulative fatigue damage. In *Proceedings of the International Conference on Fatigue of Metals*; Institution of Mechanical Engineering and American Society of Mechanical Engineers: London, UK, 1956; Volume 1, pp. 235–242.
31. Chen, X.; Jin, D.; Kim, K.S. Fatigue life prediction of type 304 stainless steel under sequential biaxial loading. *Int. J. Fatigue* **2006**, *28*, 289–299. [[CrossRef](#)]
32. Itoh, T.; Chen, X.; Nakagawa, T.; Sakane, M. A simple model for stable cyclic stress-strain relationship of type 304 stainless steel under nonproportional loading. *J. Eng. Mater. Technol. Trans. ASME* **2000**, *122*, 1–9. [[CrossRef](#)]
33. Xu, J.; Shang, D.G.; Sun, G.Q.; Chen, H.; Liu, E.T. Fatigue life prediction for GH4169 superalloy under multiaxial variable amplitude loading. *J. Beijing Univ. Technol.* **2012**, *38*, 1462–1466.
34. Freudenthal, A.M.; Heller, R.A. On stress interaction in fatigue and cumulative damage rule. *J. Aerosp. Sci.* **1959**, *26*, 431–442. [[CrossRef](#)]
35. Gao, H.; Huang, H.Z.; Zhu, S.P.; Li, Y.F.; Yuan, R. A modified nonlinear damage accumulation model for fatigue life prediction considering load interaction effects. *Sci. World J.* **2014**, *2014*, 164378. [[CrossRef](#)]
36. Yuan, R.; Li, H.; Huang, H.Z.; Zhu, S.P.; Gao, H. A nonlinear fatigue damage accumulation model considering strength degradation and its applications to fatigue reliability analysis. *Int. J. Damage Mech.* **2015**, *24*, 646–662. [[CrossRef](#)]
37. Zhou, Y.; Mu, D.S.; Han, Y.B.; Huang, X.W.; Zhang, C.C. Application of the nonlinear fatigue damage cumulative on the prediction for rail head checks initiation and wear growth. *Struct. Integr.* **2019**, *7*, 239–244. [[CrossRef](#)]
38. Kwofie, S.; Rahbar, N. An equivalent driving force model for crack growth prediction under different stress ratios. *Int. J. Fatigue* **2011**, *33*, 1199–1204. [[CrossRef](#)]

39. Kwofie, S.; Rahbar, N. A fatigue driving stress approach to damage and life prediction under variable amplitude loading. *Int. J. Damage Mech.* **2013**, *22*, 393–404. [[CrossRef](#)]
40. Zuo, F.J.; Huang, H.Z.; Zhu, S.P.; Lv, Z.; Gao, H. Fatigue life prediction under variable amplitude loading using a non-linear damage accumulation model. *Int. J. Damage Mech.* **2015**, *24*, 767–784. [[CrossRef](#)]
41. Zhu, S.P.; Hao, Y.Z.; de Oliveira Correia, J.A.; Lesiuk, G.; de Jesus, A.M. Nonlinear fatigue damage accumulation and life prediction of metals: A comparative study. *Fatigue Fract. Eng. Mater. Struct.* **2019**, *42*, 1271–1282. [[CrossRef](#)]
42. Aeran, A.; Siriwardane, S.C.; Mikkelsen, O.; Langen, I. A new nonlinear fatigue damage model based only on S-N curve parameters. *Int. J. Fatigue* **2017**, *103*, 327–341. [[CrossRef](#)]
43. Aeran, A.; Siriwardane, S.C.; Mikkelsen, O.; Langen, I. An accurate fatigue damage model for welded joints subjected to variable amplitude loading. *IOP Conf. Ser. Mater. Sci. Eng.* **2017**, *276*. [[CrossRef](#)]
44. Si-Jian, L.; Wei, L.; Da-Qing, T.; Jun-Bi, L. A new fatigue damage accumulation model considering loading history and loading sequence based on damage equivalence. *Int. J. Damage Mech.* **2018**, *27*, 707–728. [[CrossRef](#)]
45. Theil, N. Fatigue life prediction method for the practical engineering use taking in account the effect of the overload blocks. *Int. J. Fatigue* **2016**, *90*, 23–35. [[CrossRef](#)]
46. Hunter, M.S.; Fricke, W.G. Metallographic aspects of fatigue behavior of aluminum. In *American Society for Testing and Materials; AMER SOC Testing Materials 100 BARR Harbor DR: West Conshohocken, PA, USA, 1954; Volume 54*, pp. 717–736.
47. Kachele, L. *Review and Analysis of Cumulative Fatigue Damage Theories*; Technical Report August; The RAND Corporation: Santa Monica, CA, USA, 1963.
48. Leipholz, H.; Topper, T.; El Menoufy, M. Lifetime prediction for metallic components subjected to stochastic loading. *Comput. Struct.* **1983**, *16*, 499–507. [[CrossRef](#)]
49. Leipholz, H.H.E. Lifetime predictions for metallic specimens subjected to loading with varying intensity. *Mech. Mater. Struct. Theor.* **1985**, *20*, 239–246.
50. Leipholz, H. On the modified S-N curve for metal fatigue prediction and its experimental verification. *Eng. Fract. Mech.* **1986**, *23*, 495–505. [[CrossRef](#)]
51. Dowdell, D.; Leipholz, H.; Topper, T. The modified life law applied to SAE-1045 steel. *Int. J. Fract.* **1986**, *31*, 29–36. [[CrossRef](#)]
52. Spitzer, R.; Corten, H.T. Effect of Loading Sequence on Cumulative Fatigue Damage of 7075-T6 Aluminum Alloy. In *Proceedings of the American Society for Testing and Materials; ASTM: Philadelphia, PA, USA, 1956; Volume 61*, pp. 719–731.
53. Zhao, S.B. Study on the accuracy of fatigue life predictions by the generally used damage accumulation theory. *J. Mech. Strength* **2000**, *22*, 206–209.
54. Rao, J.S.; Pathak, A.; Chawla, A. Blade life: A comparison by cumulative damage theories. *J. Eng. Gas Turbines Power* **2001**, *123*, 886–892. [[CrossRef](#)]
55. Peng, Z.; Huang, H.Z.; Zhou, J.; Li, Y.F. A new cumulative fatigue damage rule based on dynamic residual S-N curve and material memory concept. *Metals* **2018**, *8*, 456. [[CrossRef](#)]
56. Jiao, J.; Lei, H.; Chen, Y.F. Numerical simulation and experimental study on constant amplitude fatigue behavior of welded cross plate-hollow sphere joints. *J. Southeast Univ. (Engl. Ed.)* **2018**, *34*, 62–70. [[CrossRef](#)]
57. Marsh, B.K.J.; Mackinnon, J.A. Random-loading and block-loading fatigue tests on sharply notched mild steel specimens. *J. Mech. Eng. Sci.* **1968**, *10*, 48–58. [[CrossRef](#)]
58. Yang, X.; Yao, W.; Duan, C. The review of ascertainable fatigue cumulative damage rule. *Eng. Sci.* **2003**, *5*, 82–87.
59. Zhu, S.p.; Huang, H.z.; Xie, L.y. Nonlinear fatigue damage cumulative model and the analysis of strength degradation based on the double parameter fatigue criterion. *China Mech. Eng.* **2008**, *19*, 2753–2761.
60. Gao, H.; Huang, H.Z.; Lv, Z.; Zuo, F.J.; Wang, H.K. An improved Corten-Dolan's model based on damage and stress state effects. *J. Mech. Sci. Technol.* **2015**, *29*, 3215–3223. [[CrossRef](#)]
61. Xue, Q.; Du, X.; Wang, S. An Improved Fatigue Life Prediction Model Based on Loading Sequence. *Zhongguo Tiedao Kexue/China Railw. Sci.* **2019**, *40*, 88–93. [[CrossRef](#)]
62. Liu, Q.; Gao, Y.; Li, Y.; Xue, Q. Fatigue life prediction based on a novel improved version of the Corten-Dolan model considering load interaction effect. *Eng. Struct.* **2020**, *221*, 111036. [[CrossRef](#)]
63. Subramanyan, S. A cumulative damage rule based on the knee point of the SN curve. *J. Eng. Mater. Technol.* **1976**, *98*, 316–321. [[CrossRef](#)]
64. Hashin, Z.; Rotem, A. A cumulative damage theory of fatigue failure. *Mater. Sci. Eng.* **1978**, *34*, 147–160. [[CrossRef](#)]
65. Pavlou, D. A phenomenological fatigue damage accumulation rule based on hardness increasing, for the 2024-T42 aluminum. *Eng. Struct.* **2002**, *24*, 1363–1368. [[CrossRef](#)]
66. Lee, Y.I.; Pan, J.; Hathaway, R.B.; Barkey, M.E. *Fatigue Testing and Analysis: Theory and Practice*; Butterworth-Heinemann: Oxford, UK, 2014.
67. El Aghoury, I.; Galal, K. A fatigue stress-life damage accumulation model for variable amplitude fatigue loading based on virtual target life. *Eng. Struct.* **2013**, *52*, 621–628. [[CrossRef](#)]
68. Rege, K.; Pavlou, D.G. A one-parameter nonlinear fatigue damage accumulation model. *Int. J. Fatigue* **2017**, *98*, 234–246. [[CrossRef](#)]
69. Zhu, S.P.; Liao, D.; Liu, Q.; Correia, J.A.; De Jesus, A.M. Nonlinear fatigue damage accumulation: Isodamage curve-based model and life prediction aspects. *Int. J. Fatigue* **2019**, *128*, 105185. [[CrossRef](#)]

70. Pavlou, D.G. The theory of the S-N fatigue damage envelope: Generalization of linear, double-linear, and non-linear fatigue damage models. *Int. J. Fatigue* **2018**, *110*, 204–214. [[CrossRef](#)]
71. Batsoulas, N.D. Cumulative Fatigue Damage: CDM-Based Engineering Rule and Life Prediction Aspect. *Steel Res. Int.* **2016**, *87*, 1670–1677. [[CrossRef](#)]
72. Xia, F.L.; Zhu, S.P.; Liao, D.; Dantas, R.; Correia, J.A.; De Jesus, A.M. Isodamage curve-based fatigue damage accumulation model considering the exhaustion of static toughness. *Eng. Fail. Anal.* **2020**, *115*, 104575. [[CrossRef](#)]
73. Ye, D.; Wang, Z. A new approach to low-cycle fatigue damage based on exhaustion of static toughness and dissipation of cyclic plastic strain energy during fatigue. *Int. J. Fatigue* **2001**, *23*, 679–687. [[CrossRef](#)]
74. Krajcinovic, D. Damage mechanics: Accomplishments, trends and needs. *Int. J. Solids Struct.* **2000**, *37*, 267–277. [[CrossRef](#)]
75. Cui, W. A state-of-the-art review on fatigue life prediction methods for metal structures. *J. Mar. Sci. Technol.* **2002**, *7*, 43–56. [[CrossRef](#)]
76. Silitonga, S.; Maljaars, J.; Soetens, F.; Snijder, H.H. Survey on damage mechanics models for fatigue life prediction. *Heron* **2013**, *58*, 25–60.
77. Kachanov, L.M. Time of the rupture process under creep conditions, *Izv. Akad. Nauk SSSR Otd. Tekh. Nauk* **1958**, *8*, 26–31.
78. Rabotnov, Y.N. Creep Problems in Structural Members. *J. Appl. Mech. Mar.* **1970**, *37*, 249. [[CrossRef](#)]
79. Chaboche, J.L. *Une loi Différentielle D'endommagement de Fatigue avec Cumulation non Linéaire*; Office Nationale d'Etudes et de Recherches Aéropatiales: Paris, France, 1974.
80. Chaboche, J.L.; Lesne, P.M. A Non-Linear Continuous Fatigue Damage Model. *Fatigue Fract. Eng. Mater. Struct.* **1988**, *11*, 1–17. [[CrossRef](#)]
81. Sun, Y.; Lu, S.; Meng, Q.; Wang, X. Online damage model of steam turbine based on continuum damage mechanics. In Proceedings of the Chinese Control Conference, CCC, Dalian, China, 26–28 July 2017; pp. 10392–10397. [[CrossRef](#)]
82. Lemaitre, J.; Plumtree, A. Application of Damage Concepts to Predict Creep-Fatigue Failures. *J. Eng. Mater. Technol.* **1979**, *101*, 284–292. [[CrossRef](#)]
83. Li, C.; Qian, Z.; Li, G. The fatigue damage criterion and evolution equation containing material microparameters. *Eng. Fract. Mech.* **1989**, *34*, 435–443. [[CrossRef](#)]
84. A continuum damage model for weld heat affected zone under low cycle fatigue loading. *Eng. Fract. Mech.* **1990**, *37*, 825–829. [[CrossRef](#)]
85. June, W. A continuum damage mechanics model for low-cycle fatigue failure of metals. *Eng. Fract. Mech.* **1992**, *41*, 437–441. [[CrossRef](#)]
86. Cheng, G.; Plumtree, A. A fatigue damage accumulation model based on continuum damage mechanics and ductility exhaustion. *Int. J. Fatigue* **1998**, *20*, 495–501. [[CrossRef](#)]
87. Shang, D.G.G.; Yao, W.X.X. A nonlinear damage cumulative model for uniaxial fatigue. *Int. J. Fatigue* **1999**, *21*, 187–194. [[CrossRef](#)]
88. Salomón, O.; Oñate, E.; Oller, S.; Car, E. Thermomechanical Fatigue Analysis Based on Continuum Mechanics. *Mecánica Computacional* **1999**, *3*, 133–143.
89. Oller, S. Thermo-mechanical fatigue analysis using generalized continuum damage mechanics and the finite element method. *Int. J. Numer. Methods Eng.* **2001**, 1–22. Available online: http://150.107.117.36/NPTEL_DISK4/NPTEL_Contents/Web_courses/Phase2_web/105108072/mod08/application-3.pdf (accessed on 20 January 2020).
90. Salomón, O.; Oller, S.; Oñate, E. Fatigue analysis of materials and structures using continuum damage model. *Int. J. Form. Process.* **2002**, *5*, 493–503. [[CrossRef](#)]
91. Oller, S.; Salomón, O.; Oñate, E. A continuum mechanics model for mechanical fatigue analysis. *Comput. Mater. Sci.* **2005**, *32*, 175–195. [[CrossRef](#)]
92. Dattoma, V.; Giancane, S.; Nobile, R.; Panella, F.W. Fatigue life prediction under variable loading based on a new non-linear continuum damage mechanics model. *Int. J. Fatigue* **2006**, *28*, 89–95. [[CrossRef](#)]
93. Giancane, S.; Nobile, R.; Panella, F.W.; Dattoma, V. Fatigue life prediction of notched components based on a new nonlinear continuum damage mechanics model. *Procedia Eng.* **2010**, *2*, 1317–1325. [[CrossRef](#)]
94. Zhang, J.; Fu, X.; Lin, J.; Liu, Z.; Liu, N.; Wu, B. Study on damage accumulation and life prediction with loads below fatigue limit based on a modified nonlinear model. *Materials* **2018**, *11*, 2298. [[CrossRef](#)]
95. Sinclair, G. *An Investigation of the Coaxing Effect in Fatigue of Metals*; Technical Report; Illinois University at Urbana: Urbana, IL, USA, 1952.
96. Xi, L.; Songlin, Z. Strengthening of transmission gear under low-amplitude loads. *Mater. Sci. Eng. A* **2008**, *488*, 55–63. [[CrossRef](#)]
97. Xi, L.; Songlin, Z. Changes in mechanical properties of vehicle components after strengthening under low-amplitude loads below the fatigue limit. *Fatigue Fract. Eng. Mater. Struct.* **2009**, *32*, 847–855. [[CrossRef](#)]
98. Bhattacharya, B.; Ellingwood, B. *A Damage Mechanics Based Approach to Structural Deterioration and Reliability*; Nuclear Regulatory Commission: Washington, DC, USA, 1998.
99. Bhattacharya, B.; Ellingwood, B. A new CDM-based approach to structural deterioration. *Int. J. Solids Struct.* **1999**, *36*, 1757–1779. [[CrossRef](#)]
100. Li, Z.X.; Chan, T.H.; Ko, J.M. Fatigue damage model for bridge under traffic loading: Application made to Tsing Ma Bridge. *Theor. Appl. Fract. Mech.* **2001**, *35*, 81–91. [[CrossRef](#)]

101. Krajcinovic, D.; Lemaitre, J. *Continuum Damage Mechanics: Theory and Applications*; Springer: Berlin/Heidelberg, Germany, 1987; pp. 75–81.
102. Li, Z.X.; Ko, J.M.; Chan, T.H. Modelling of load interaction and overload effect on fatigue damage of steel bridges. *Fatigue Fract. Eng. Mater. Struct.* **2001**, *24*, 379–390. [[CrossRef](#)]
103. Li, Z.X.; Chan, T.H.; Ko, J.M. Fatigue analysis and life prediction of bridges with structural health monitoring data—Part I: Methodology and strategy. *Int. J. Fatigue* **2001**, *23*, 45–53. [[CrossRef](#)]
104. Chan, T.H.; Li, Z.X.; Ko, J.M. Fatigue analysis and life prediction of bridges with structural health monitoring data—Part II: Application. *Int. J. Fatigue* **2001**, *23*, 55–64. [[CrossRef](#)]
105. Li, Z.X.; Chan, T.H.; Ko, J.M. Evaluation of typhoon induced fatigue damage for Tsing Ma Bridge. *Eng. Struct.* **2002**, *24*, 1035–1047. [[CrossRef](#)]
106. Xu, Y.L.; Liu, T.T.; Zhang, W.S. Buffeting-induced fatigue damage assessment of a long suspension bridge. *Int. J. Fatigue* **2009**, *31*, 575–586. [[CrossRef](#)]
107. Xu, Y.L.; Chen, Z.W.; Xia, Y. Fatigue assessment of multi-loading suspension bridges using continuum damage model. *Int. J. Fatigue* **2012**, *40*, 27–35. [[CrossRef](#)]
108. Wang, H.; Qin, S.; Wang, Y. Nonlinear cumulative damage model and application to bridge fatigue life evaluation. *Adv. Struct. Eng.* **2018**, *21*, 1402–1408. [[CrossRef](#)]
109. Mesmacque, G.; Garcia, S.; Amrouche, A.; Rubio-Gonzalez, C. Sequential law in multiaxial fatigue, a new damage indicator. *Int. J. Fatigue* **2005**, *27*, 461–467. [[CrossRef](#)]
110. Aid, A.; Amrouche, A.; Bouiadjra, B.B.; Benguediab, M.; Mesmacque, G. Fatigue life prediction under variable loading based on a new damage model. *Mater. Des.* **2011**, *32*, 183–191. [[CrossRef](#)]
111. Siriwardane, S.; Ohga, M.; Dissanayake, R.; Taniwaki, K. Application of new damage indicator-based sequential law for remaining fatigue life estimation of railway bridges. *J. Constr. Steel Res.* **2008**, *64*, 228–237. [[CrossRef](#)]
112. Adasooriya, N.D.; Siriwardane, S.C. Remaining fatigue life estimation of corroded bridge members. *Fatigue Fract. Eng. Mater. Struct.* **2014**, *37*, 603–622. [[CrossRef](#)]
113. Aid, A.; Bendouba, M.; Aminallah, L.; Amrouche, A.; Benseddiq, N.; Benguediab, M. An equivalent stress process for fatigue life estimation under multiaxial loadings based on a new non linear damage model. *Mater. Sci. Eng. A* **2012**, *538*, 20–27. [[CrossRef](#)]
114. Pitoiset, X.; Preumont, A. Spectral methods for multiaxial random fatigue analysis of metallic structures. *Int. J. Fatigue* **2000**, *22*, 541–550. [[CrossRef](#)]
115. Sines, G. Behavior of metals under complex static and alternating stresses. *Met. Fatigue* **1959**, *1*, 145–169.
116. Crossland, B. Effect of large hydrostatic pressures on the torsional fatigue strength of an alloy steel. In *Proceedings of the International Conference on Fatigue of Metals*, London, UK, 10–14 September 1956; Institution of Mechanical Engineers: London, UK, 1956; Volume 138, p. 12.
117. Bannantine, J.A.; Socie, D.F. A variable amplitude multiaxial fatigue life prediction method. In *Proceedings of the Thirth International Conference on Biaxial/Multiaxial Fatigue*; Universität Stuttgart: Stuttgart, Germany, 1989; pp. 12.1–12.20.
118. Fatemi, A.; Socie, D.F. A critical plane approach to multiaxial fatigue damage including out-of-phase loading. *Fatigue Fract. Eng. Mater. Struct.* **1988**, *11*, 149–165. [[CrossRef](#)]
119. Socie, D. Critical plane approaches for multiaxial fatigue damage assessment. In *Advances in Multiaxial Fatigue*; ASTM International: West Conshohocken, PA, USA, 1993.
120. Wang, C.H.; Brown, M.W. A Path-Independent Parameter for Fatigue Under Proportional and Non-Proportional Loading. *Fatigue Fract. Eng. Mater. Struct.* **1993**, *16*, 1285–1297. [[CrossRef](#)]
121. Lagoda, T.; Macha, E.; Bedkowski, W.X. A critical plane approach based on energy concepts: Application to biaxial random tension-compression high-cycle fatigue regime. *Int. J. Fatigue* **1999**, *21*, 431–443. [[CrossRef](#)]
122. Benkabouche, S.; Guechichi, H.; Amrouche, A.; Benkhettab, M. A modified nonlinear fatigue damage accumulation model under multiaxial variable amplitude loading. *Int. J. Mech. Sci.* **2015**, *100*, 180–194. [[CrossRef](#)]
123. Shen, C.; Talha, A.; Hamdi, A.; Benseddiq, N. A new cumulative fatigue damage model under biaxial loading. *Proc. Inst. Mech. Eng. Part L J. Mater. Des. Appl.* **2020**, *234*, 962–973. [[CrossRef](#)]
124. Robert, J.L. Contribution à L'étude de la Fatigue Multi Axiale sous Sollicitations Periodiques ou Aléatoires. Ph.D. Thesis, Institut National des Sciences Appliquées, Lyon, France, 1992.
125. Dang Van, K. *Sur la Résistance à la Fatigue des Métaux*. Ph.D. Thesis, Science et Techniques de l'Armement 3ème Fascicule, Paris, France, 1973.
126. Weber, B. Fatigue Multiaxiale des Structures Industrielles sous Chargement Quelconque. Ph.D. Thesis, L'Institut National des Sciences Appliquées, Lyon, France, 1999.
127. Ye, D.; Wang, Z. Change characteristics of static mechanical property parameters and dislocation structures of 45# medium carbon structural steel during fatigue failure process. *Mater. Sci. Eng. A* **2001**, *297*, 54–61. [[CrossRef](#)]
128. Cadenas, P.; Amrouche, A.; Mesmacque, G.; Jozwiak, K. Effect of the residual fatigue damage on the static and toughness properties. In *Damage and Fracture Mechanics: Failure Analysis of Engineering Materials and Structures*; Springer: Berlin/Heidelberg, Germany, 2009; pp. 323–330. [[CrossRef](#)]
129. Lv, Z.; Huang, H.Z.; Zhu, S.P.; Gao, H.; Zuo, F. A modified nonlinear fatigue damage accumulation model. *Int. J. Damage Mech.* **2014**, *24*, 168–181. [[CrossRef](#)]

130. Morrow, J.D. The effect of selected sub-cycle sequences in fatigue loading histories. *Random Fatigue Life Predict.* **1986**, *72*, 43–60.
131. Böhm, E.; Kurek, M.; Junak, G.; Cieśla, M.; Łagoda, T. Accumulation of Fatigue Damage Using Memory of the Material. *Procedia Mater. Sci.* **2014**, *3*, 2–7. [[CrossRef](#)]
132. Böhm, E.; Kurek, M.; Łagoda, T. Accumulation of fatigue damages for block-type loads with use of material memory function. *Solid State Phenom.* **2015**, *224*, 39–44. [[CrossRef](#)]
133. Zhou, J.; Huang, H.Z.; Barnhart, M.V.; Huang, G.; Li, Y.F. A novel non-linear cumulative fatigue damage model based on the degradation of material memory. *Int. J. Damage Mech.* **2020**, *29*, 610–625. [[CrossRef](#)]
134. Lefebvre, D.; Neale, K.W.; Ellyin, F. A criterion for low-cycle fatigue failure under biaxial states of stress. *J. Eng. Mater. Technol. Trans. ASME* **1981**, *103*, 1–6. [[CrossRef](#)]
135. Kujawski, D.; Ellyin, F. A cumulative damage theory for fatigue crack initiation and propagation. *Int. J. Fatigue* **1984**, *6*, 83–88. [[CrossRef](#)]
136. Ellyin, F.; Kujawski, D. An energy-based fatigue failure criterion. *Microstruct. Mech. Behav. Mater.* **1985**, *2*, 591–600.
137. Golos, K.; Ellyin, F. Generalization of cumulative damage criterion to multilevel cyclic loading. *Theor. Appl. Fract. Mech.* **1987**, *7*, 169–176. [[CrossRef](#)]
138. Ellyin, F. Fatigue Life Prediction Under Multiaxial Stress Conditions. *Developments in Engineering Mechanics*; Selvadurai, A.P.S., Ed.; Elsevier Science Publishers BV: Amsterdam, The Netherlands, 1987; pp. 133–158.
139. Golos, K.; Ellyin, F. A Total Strain Energy Density Theory for Cumulative Fatigue Damage. *J. Press. Vessel. Technol.* **1988**, *110*, 36. [[CrossRef](#)]
140. Park, S.H.; Hong, S.G.; Lee, B.H.; Lee, C.S. Fatigue life prediction of rolled AZ31 magnesium alloy using an energy-based model. *Int. J. Mod. Phys. B* **2008**, *22*, 5503–5508. [[CrossRef](#)]
141. Ellyin, F.; Golos, K. Multiaxial fatigue damage criterion. *J. Eng. Mater. Technol.* **1988**, *110*, 63–68. [[CrossRef](#)]
142. Macha, E.; Sonsino, C.M. Energy criteria of multiaxial fatigue failure. *Fatigue Fract. Eng. Mater. Struct.* **1999**, *22*, 1053–1070. [[CrossRef](#)]
143. Łagoda, T. Energy models for fatigue life estimation under uniaxial random loading. Part I: The model elaboration. *Int. J. Fatigue* **2001**, *23*, 467–480. [[CrossRef](#)]
144. Łagoda, T. Energy models for fatigue life estimation under uniaxial random loading. Part II: Verification of the model. *Int. J. Fatigue* **2001**, *23*, 481–489. [[CrossRef](#)]
145. Jahed, H.; Varvani-Farahani, A. Upper and lower fatigue life limits model using energy-based fatigue properties. *Int. J. Fatigue* **2006**, *28*, 467–473. [[CrossRef](#)]
146. Jahed, H.; Varvani-Farahani, A.; Noban, M.; Khalaji, I. An energy-based fatigue life assessment model for various metallic materials under proportional and non-proportional loading conditions. *Int. J. Fatigue* **2007**, *29*, 647–655. [[CrossRef](#)]
147. Gu, Z.; Mi, C.; Ding, Z.; Zhang, Y.; Liu, S.; Nie, D. An energy-based fatigue life prediction of a mining truck welded frame. *J. Mech. Sci. Technol.* **2016**, *30*, 3615–3624. [[CrossRef](#)]
148. Scott-Emuakpor, O.; Herman Shen, M.H.; Cross, C.; Calcatera, J.; George, T. Development of an improved high cycle fatigue criterion. In *ASME Turbo Expo*; ASME: Vienna, Austria, 2004; pp. 1–8. [[CrossRef](#)]
149. Scott-Emuakpor, O.; Herman Shen, M.H.; Cross, C.; Calcatera, J.; George, T. A promising new energy-based fatigue life prediction framework. *Proc. ASME Turbo Expo* **2005**, *4*, 397–404. [[CrossRef](#)]
150. Scott-Emuakpor, O.; Shen, M.H.; George, T.; Cross, C.J.; Calcatera, J. Development of an improved high cycle fatigue criterion. *J. Eng. Gas Turbines Power* **2007**, *129*, 162–169. [[CrossRef](#)]
151. Scott-Emuakpor, O.E. Development of a Novel Energy-Based Method for Multi-Axial Fatigue Strength Assessment. Ph.D. Thesis, The Ohio State University, Columbus, OH, USA, 2007.
152. Scott-Emuakpor, O.E.; Shen, H.; George, T.; Cross, C. An energy-based uniaxial fatigue life prediction method for commonly used gas turbine engine materials. *J. Eng. Gas Turbines Power* **2008**, *130*, 062504. [[CrossRef](#)]
153. Papadopoulos, I.V.; Panoskaltsis, V.P. Invariant formulation of a gradient dependent multiaxial high-cycle fatigue criterion. *Eng. Fract. Mech.* **1996**, *55*, 513–528. [[CrossRef](#)]
154. Stowell, E.Z. A study of the energy criterion for fatigue. *Nucl. Eng. Des.* **1966**, *3*, 32–40. [[CrossRef](#)]
155. Scott-Emuakpor, O.; George, T.; Cross, C.; Shen, M.H. Multi-axial fatigue-life prediction via a strain-energy method. *AIAA J.* **2010**, *48*, 63–72. [[CrossRef](#)]
156. Feltner, C.E.; Morrow, J.D. Microplastic strain hysteresis energy as a criterion for fatigue fracture. *J. Fluids Eng. Trans. ASME* **1961**, *83*, 15–22. [[CrossRef](#)]
157. Ozaltun, H.; Shen, M.H.; George, T.; Cross, C. An Energy Based Fatigue Life Prediction Framework for In-Service Structural Components. *Exp. Mech.* **2011**, *51*, 707–718. [[CrossRef](#)]
158. Wertz, J.; Shen, M.H.; Scott-Emuakpor, O.; George, T.; Cross, C. An Energy-Based Torsional-Shear Fatigue Lifting Method. *Exp. Mech.* **2012**, *52*, 705–715. [[CrossRef](#)]
159. Letcher, T.; Shen, M.H.; Scott-Emuakpor, O.; George, T.; Cross, C. An energy-based critical fatigue life prediction method for AL6061-T6. *Fatigue Fract. Eng. Mater. Struct.* **2012**, *35*, 861–870. [[CrossRef](#)]
160. Djebli, A.; Aid, A.; Bendouba, M.; Amrouche, A.; Benguediab, M.; Benseddiq, N. A non-linear energy model of fatigue damage accumulation and its verification for Al-2024 aluminum alloy. *Int. J. Non-Linear Mech.* **2013**, *51*, 145–151. [[CrossRef](#)]

161. Peng, Z.; Huang, H.Z.; Zhu, S.P.; Gao, H.; Lv, Z. A fatigue driving energy approach to high-cycle fatigue life estimation under variable amplitude loading. *Fatigue Fract. Eng. Mater. Struct.* **2016**, *39*, 180–193. [[CrossRef](#)]
162. Patil, N.; Mahadevan, P.; Chatterjee, A. A constructive empirical theory for metal fatigue under block cyclic loading. *Proc. R. Soc. A Math. Phys. Eng. Sci.* **2008**, *464*, 1161–1179. [[CrossRef](#)]
163. Taheri, S. Invalidation de quelques méthodes de cumul de dommage non linéaire en favor d'un cumul linéaire. In *Proceedings of Fatigue Design*; Cetim: Senlis, France, 2007.
164. Colin, J.; Fatemi, A.; Taheri, S. Fatigue behavior of stainless steel 304L including strain hardening, prestraining, and mean stress effects. *J. Eng. Mater. Technol. Trans. ASME* **2010**, *132*, 0210081–02100813. [[CrossRef](#)]
165. Colin, J.; Fatemi, A.; Taheri, S. Cyclic hardening and fatigue behavior of stainless steel 304L. *J. Mater. Sci.* **2011**, *46*, 145–154. [[CrossRef](#)]
166. Taheri, S.; Vincent, L.; Le-Roux, J.C. A new model for fatigue damage accumulation of austenitic stainless steel under variable amplitude loading. *Procedia Eng.* **2013**, *66*, 575–586. [[CrossRef](#)]